

alkoxide reaction. The reaction of $(C_5H_5)_2YCl(THF)$ with $KOMe \cdot MeOH$ also generates an oxide in the product, $(C_5H_5)_2Y_2(\mu-OMe)_4(\mu_3-OMe)_4O$,¹² and we currently are investigating other examples of this phenomena which we have observed.

Li vs Na Countercations. There are numerous examples in organoyttrium and organolanthanide chemistry in which the presence and specific nature of the cation strongly influences the chemistry.^{2,57,58} Hence, it is not unreasonable to see different results in the $NaOCMe_3$ vs $LiOCMe_3$ reactions. Given the complexity of the $LiOCMe_3$ reactions compared to the $NaOCMe_3$ systems and the presence of several lithium atoms in **3**, it appears the lithium is more readily carried along in these systems. This leads to a wider variety of products and crystallographically more difficult systems.

Conclusions

The reactions of YCl_3 and $LaCl_3$ with alkali metal alkoxides have provided a new and important class of polylanthanide and polyyttrium alkoxide and oxide complexes. Despite the structural complexity of these complexes it has proven possible to correlate X-ray and ¹H NMR data to allow this chemistry to be followed

and monitored by NMR spectroscopy. When several of these complexes are viewed together structural correlations become evident. Most important is the existence of $Ln_3(\mu_3-OR)(\mu_3-X)(\mu-OR)_3$ building blocks from which a variety of structures can be constructed. Since our study used metals representative of both the early (La) and late (Y) lanthanides, this chemistry is likely to be general in the series. These alkoxide complexes have demonstrated that the $OCMe_3$ ligand can be used as a viable replacement for C_5H_5 groups. Given the importance of C_5H_5 as a co-ligand in mono- and bimetallic lanthanide and yttrium organometallic chemistry, it is likely that the $OCMe_3$ ligand will find a similarly important place in the tri- and polymetallic chemistry of these metals. Continued efforts in this area will concentrate on preparing alkyl and hydride derivatives of these and related species.

Acknowledgment. We thank the Division of Chemical Sciences of the Office of Basic Energy Sciences of the Department of Energy for support of the research and Professor R. J. Doedens for his help and advice with the crystal structure determinations.

Registry No. 1, 112596-07-3; 2, 112710-05-1; 3, 112596-10-8; 4, 112596-08-4.

Supplementary Material Available: A fully-numbered ORTEP plot of **1** plus tables of complete bond distances and angles and thermal parameters (9 pages); listings of observed and calculated structure factors for **1** and **3** (25 pages). Ordering information is given on any current masthead page.

(57) Tilley, T. D.; Andersen, R. A.; Spencer, B.; Ruben, H.; Zalkin, A.; Templeton, D. H. *Inorg. Chem.* **1980**, *19*, 2999-3003.

(58) References 9 and 35. Schumann, H.; Genthe, W. *J. Organomet. Chem.* **1981**, *213*, C7-C9. Schumann, H.; Genthe, W.; Hahn, E.; Hossain, M. B.; van der Helm, D. *J. Organomet. Chem.* **1986**, *299*, 67-84.

Angle Dependence of the Properties of the $[Fe_2X]^{4+}$ Bridge Unit (X = O, S): Structures, Antiferromagnetic Coupling, and Properties in Solution

R. N. Mukherjee, T. D. P. Stack, and R. H. Holm*

Contribution from the Department of Chemistry, Harvard University, Cambridge, Massachusetts 02138. Received June 26, 1987

Abstract: The effects of changing the bridge angle θ in the bridges $Fe(III)-X-Fe(III)$ (X = O, S) as they occur in complexes of the type $[Fe(salen)]_2X$ (salen = 1,2-bis(salicylideneamino)ethane(2-)) have been investigated. The method employed involves escalating steric repulsions between half-dimers by introduction of *t*-Bu groups at ring 3-positions and four methyl groups on the ethylene bridge, affording the complexes $[Fe(3-tBuSalmen)]_2X$ (X = O (**6**), S (**7**)). Complex **6** (**7**) crystallizes in monoclinic space group $P2_1/a$ with $a = 20.395$ (3) Å, $b = 11.864$ (3) Å, $c = 24.311$ (4) Å, $\beta = 114.61$ (1)° ($a = 20.931$ (8) Å, $b = 11.884$ (6) Å, $c = 24.229$ (7) Å, $\beta = 114.34$ (2)°), and $Z = 4$. On the basis of 4417 (3642) unique data with $F_o^2 > 2.5 \sigma(F_o^2)$, the structures were refined to $R = 5.8$ (6.5)%. Bridge angles of 173.4 (2)° (**6**) and 167.0 (2)° (**7**) are markedly larger than those of $[Fe(salen)]_2O$ (**8**, 145°) and $[Fe(salen)]_2S$ (**9**, 122°) determined earlier; these complexes have much weaker steric interactions between half-dimers. A scheme for defining the configurations of these molecules in terms of θ and conformational angles $[\Omega_1, \Omega_2]$ is introduced. Antiferromagnetic coupling shows a small but definite increase as θ increases: $J = -183$ (**8**) and -200 (**6**) cm^{-1} and $J = -178$ (**9**) and -218 (**7**) cm^{-1} . Bridge Fe-O distances in **6** and **8** are indistinguishable, and thus are not a factor in regulating coupling. J values for **6** and **7** provide the best current evidence that at nearly constant θ values, antiferromagnetic coupling is transmitted more effectively by a sulfido than an oxo bridge. Analysis of magnetic data in solution and determination of hyperfine coupling constants from contact shifts indicates that **6** and **8** retain their solid-state structures in solution and that the larger shifts of **9** versus **8** arise mainly from susceptibility differences, which are primarily controlled by bridge angle. Molecular configurations of **6-9** as well as those of recently reported $[Fe(acen)]_2X$ (X = O, S; acen = *N,N'*-ethylenebis(acetylacetonate)iminato(2-)) are predicted within small limits of angular parameters by a van der Waals potential function for intramolecular interactions. Calculations at the extended Hückel level indicate a small preference for a linear and bent bridge ($\theta = 135-140^\circ$) for X = O and S, respectively, at the crystallographically determined conformational angles. Non-bonded repulsions evidently override the linear oxo bridge preference and reinforce the bent sulfido bridge preference. The increase in J values with increasing θ can be rationalized in terms of a MO model of antiferromagnetic coupling with an important π -super-exchange pathway.

A fundamental structural component of the chemistry of Fe(III) is the μ -oxo bridge unit $Fe-O-Fe$,¹ which is known to occur with variable bridge angles in the range 139-180° but always with

antiferromagnetically coupled Fe atoms. The bridge is usually found in the unsupported condition, i.e., in the absence of other bridges. $[Fe(salen)]_2O$ and related compounds (salen = 1,2-bis(salicylideneamino)ethane) are familiar examples of unsupported bridges. This bridge unit also arises in the supported mode.

(1) Murray, K. S. *Coord. Chem. Rev.* **1974**, *12*, 1.

Notably important examples are found in methemerythrin,² ribonucleotide reductase,³ and model compounds⁴ in which two $\mu_2\text{-RCO}_2^-$ groups support the oxo bridges. In these cases the carboxylate bridge interactions apparently serve to decrease the Fe–O–Fe bridge angle (123–128°) and enhance somewhat the magnetic exchange interactions.

The isoelectronic Fe–S–Fe bridge unit is known in only two compounds and only in the unsupported condition. The first example of a complex with this unit was $[\text{Fe}(\text{salen})_2]\text{S}$, prepared independently in 1973.^{5,6} Subsequently, it was synthesized in a different way in this laboratory and shown to be antiferromagnetic with a bridge angle of 122°.⁷ Very recently, the complexes $[\text{Fe}(\text{acen})_2]\text{X}$ (X = O, S) have been reported and shown by X-ray diffraction to contain unsupported bridges.⁸ The Fe–S–Fe unit assumes special significance because in various supported modes it is a fragment of all structurally defined iron–sulfur clusters. This group of clusters includes the core units $[\text{Fe}_2\text{S}_2]^{2+}$,⁹ $[\text{Fe}_3\text{S}_4]^+$,¹⁰ $[\text{Fe}_4\text{S}_4]^{3+,2+,+}$,^{9,11} $[\text{Fe}_6\text{S}_6]^{4+,3+,}$,^{12,13} $[\text{Fe}_6\text{S}_8]^{2+,+}$,¹⁴ $[\text{Fe}_6\text{S}_9]^{4-}$,^{10,15} $[\text{Fe}_7\text{S}_7]^{3+,16}$ and $[\text{Fe}_8\text{S}_8]^{5+,17}$ with doubly, triply, or quadruply bridging sulfur atoms. These units exhibit delocalized electronic structures and magnetic properties indicative of dominant antiferromagnetic coupling. In all cases, Fe atoms are bridged by two or more sulfur atoms. It is possible that the magnetic interactions occur mainly via a superexchange pathway through the sulfur atoms, with some contribution from direct metal–metal exchange. Iron atom separations in these clusters are in the 2.6–2.8-Å range. Magnetic interactions between metal atoms through sulfur-containing ligands have been summarized.¹⁸

In the $[\text{Fe}(\text{salen})_2]\text{O}$ series bridge angles are 139–144°.^{19–22} Substantially larger angles are found in two μ -oxo bis[bis(salicylaldiminato)iron(III)] complexes (164°,²³ 175°²⁴) in which the

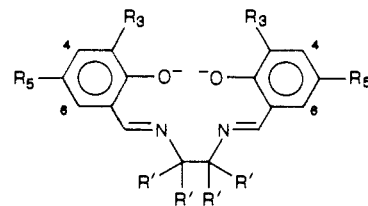
ligands in the half-dimers have the trans arrangement with consequent changes in nonbonded interactions between the halves versus those in $[\text{Fe}(\text{salen})_2]\text{O}$.

The foregoing results suggest that while Fe–S–Fe bridge angles are likely always to be smaller than Fe–O–Fe angles with the same ligand structure, both may be subjected to manipulation by adjusting nonbonded repulsions. If so, this would permit several significant aspects of unsupported bridges to be addressed experimentally: (i) oxo and sulfido bridge angle differences under steric stress at parity of ligand structure, with particular reference to the tendency of the smaller sulfido angle to enlarge; (ii) relative extents of antiferromagnetic interactions through oxo and sulfido bridging atoms as dependent on bridge angles. In addition, other potentially angle-dependent properties could be probed. The analysis by Hay et al.²⁵ of antiferromagnetic contributions to magnetic exchange in dimers implies an angle dependence of the coupling constant J . Antiferromagnetism is well established for members of the $[\text{Fe}(\text{salen})_2]\text{O}$ series^{1,26} and related Schiff base Fe(III) complexes.²⁷

We have undertaken an investigation of the angular deformability of $[\text{Fe}_2\text{X}]^{4+}$ bridge units (X = O, S) and the modulation of properties therewith, particularly antiferromagnetic exchange interactions. This work includes a more detailed study of the $[\text{Fe}_2\text{S}]^{4+}$ bridge unit in salen-type complexes than presented earlier,⁷ including demonstration that it and the unit $[\text{Fe}_2\text{O}]^{4+}$ are susceptible to large angular deformations under steric tension and that antiferromagnetic interactions are demonstrably dependent on bridge angle. Also included are investigations related to solution structures and molecular conformations, calculations of electronic structures and energies as a function of bridge angle, and reexamination of several solution properties reported in our initial study of $[\text{Fe}(\text{salen})_2]\text{S}$.⁷ The broad purpose of this and our earlier work is to develop a profile of comparative properties of the $[\text{Fe}_2\text{X}]^{4+}$ groups and a more thorough definition of the $[\text{Fe}_2\text{S}]^{4+}$ group itself, just as has been done for certain of the polynuclear Fe–S core units above.

Experimental Section

Preparation of Compounds. Substituted salicylaldehydes were obtained from the appropriate phenols by the Duff reaction,²⁸ 2,3-Diamino-2,3-dimethylbutane was prepared by the method of Sayre.²⁹ The Schiff bases 1,2-bis(5-*tert*-butylsalicylideneamino)ethane ($\text{H}_2(5\text{-}t\text{Busalen})$, **2**) and 2,3-dimethyl-2,3-bis(3-*tert*-butylsalicylideneamino)butane ($\text{H}_2(3\text{-}t\text{Busaltmen})$, **3**) were prepared by stoichiometric reactions of the salicylaldehyde and diamine in methanol. The crude solids were recrystallized from methanol to afford yellow crystalline products that were shown to be pure by their ¹H NMR spectra. Anhydrous iron(II) acetate was prepared under anaerobic conditions by a reported method.³⁰ All solvents were dried before use in the preparations which follow. All manipulations were performed under a pure dinitrogen atmosphere unless noted otherwise. Ligand structures and abbreviations are indicated below.



salen (**1**): $\text{R}_3 = \text{R}_5 = \text{H}$
 5-*t*Busalen (**2**): $\text{R}_3 = \text{H}$, $\text{R}_5 = t\text{Bu}$
 3-*t*Busaltmen (**3**): $\text{R}_3 = t\text{Bu}$, $\text{R}_5 = \text{H}$, $\text{R}' = \text{Me}$

- (2) Stenkamp, R. E.; Sieker, L. C.; Jensen, L. H. *J. Am. Chem. Soc.* **1984**, *106*, 618.
 (3) Scarrow, R. C.; Maroney, M. J.; Palmer, S. M.; Que, L., Jr.; Salowe, S. P.; Stubbe, J. *J. Am. Chem. Soc.* **1986**, *108*, 6832.
 (4) (a) Armstrong, W. H.; Spool, A.; Papaefthymiou, G. C.; Frankel, R. B.; Lippard, S. J. *J. Am. Chem. Soc.* **1984**, *106*, 3653. (b) Wiegardt, K.; Pohl, K. *Angew. Chem., Int. Ed. Engl.* **1983**, *22*, 727. (c) Armstrong, W. H.; Lippard, S. J. *J. Am. Chem. Soc.* **1983**, *105*, 4837. (d) See also: Armstrong, W. H.; Lippard, S. J. *J. Am. Chem. Soc.* **1985**, *107*, 3730.
 (5) Mitchell, P. C. H.; Parker, D. A. *J. Inorg. Nucl. Chem.* **1973**, *35*, 1385.
 (6) Floriani, C.; Fachinetti, G. *Gazz. Chim. Ital.* **1973**, *103*, 1317.
 (7) Dorfman, J. R.; Girerd, J.-J.; Simhon, E. D.; Stack, T. D. P.; Holm, R. H. *Inorg. Chem.* **1984**, *23*, 4407.
 (8) Corazza, F.; Floriani, C.; Zehnder, M. *J. Chem. Soc., Dalton Trans.* **1987**, 709.
 (9) Berg, J. M.; Holm, R. H. In *Metals Ions in Biology*; Spiro, T. G., Ed.; Interscience: New York, 1982; Vol. 4, Chapter 1.
 (10) Hagen, K. S.; Watson, A. D.; Holm, R. H. *J. Am. Chem. Soc.* **1983**, *105*, 3905.
 (11) O'Sullivan, T.; Millar, M. M. *J. Am. Chem. Soc.* **1985**, *107*, 4096.
 (12) (a) Kanatzidis, M. G.; Hagen, W. R.; Dunham, W. R.; Lester, R. K.; Coucouvanis, D. *J. Am. Chem. Soc.* **1985**, *107*, 953. (b) Kanatzidis, M. G.; Salifoglu, A.; Coucouvanis, D. *Inorg. Chem.* **1986**, *25*, 2460.
 (13) Saak, W.; Henkel, G.; Pohl, S. *Angew. Chem., Int. Ed. Engl.* **1984**, *23*, 150.
 (14) (a) Agresti, A.; Bacci, M.; Cecconi, F.; Ghilardi, C. A.; Midollini, S. *Inorg. Chim.* **1985**, *24*, 689. (b) Cecconi, F.; Ghilardi, C. A.; Midollini, S.; Orlandini, A.; Zanello, P. *J. Chem. Soc., Dalton Trans.* **1987**, 831.
 (15) (a) Christou, G.; Sabat, M.; Ibers, J. A.; Holm, R. H. *Inorg. Chem.* **1982**, *21*, 3518. (b) Strasdeit, H.; Krebs, B.; Henkel, G. *Inorg. Chem.* **1984**, *23*, 1816.
 (16) Noda, I.; Synder, B. S.; Holm, R. H. *Inorg. Chem.* **1986**, *25*, 3851.
 (17) Pohl, S.; Saak, W. *Angew. Chem., Int. Ed. Engl.* **1984**, *23*, 907.
 (18) Kahn, O.; Girerd, J.-J. In *Sulfur: Its Significance for Chemistry, for the Geo-, Bio-, and Cosmospere and Technology*; Müller, A.; Krebs, B., Eds.; Elsevier: New York, 1984; pp 195–220.
 (19) Calligaris, M.; Nardin, G.; Randaccio, L. *Coord. Chem. Rev.* **1972**, *7*, 385.
 (20) Gerloch, M.; McKenzie, E. D.; Towl, A. D. C. *J. Chem. Soc. A* **1969**, 2850.
 (21) Coggon, P.; McPhail, A. T.; Mabbs, F. E. *J. Chem. Soc. A* **1971**, 1014.
 (22) Davies, J. E.; Gatehouse, B. M. *Acta Crystallogr.* **1973**, *B29*, 1934.

- (23) Davies, J. E.; Gatehouse, B. M. *Cryst. Struct. Commun.* **1972**, *1*, 115.
 (24) Davies, J. E.; Gatehouse, B. M. *Acta Crystallogr.* **1973**, *B29*, 2651.
 (25) Hay, P. J.; Thibeault, J. C.; Hoffmann, R. *J. Am. Chem. Soc.* **1975**, *97*, 4884.
 (26) Wollman, R. G.; Hendrickson, D. N. *Inorg. Chem.* **1977**, *16*, 723.
 (27) van den Bergen, A.; Murray, K. S.; O'Connor, M. J.; Rehak, N.; West, B. O. *Aust. J. Chem.* **1968**, *21*, 1517.
 (28) Duff, J. C. *J. Chem. Soc.* **1941**, 547.
 (29) (a) Sayre, R. *J. Am. Chem. Soc.* **1955**, *77*, 6689. (b) See also: Averill, D. F.; Broman, R. F. *Inorg. Chem.* **1978**, *17*, 3389.
 (30) Earnshaw, A.; King, E. A.; Larkworthy, L. F. *J. Chem. Soc. A* **1968**, 1048.

(a) [Fe(5-*t*-Busalen)]₂O (4). To a stirred solution of 2.00 g (5.26 mmol) of H₂(5-*t*-Busalen) in 30 mL of acetonitrile was added 0.92 g (5.29 mmol) of anhydrous Fe(OAc)₂. The mixture, which rapidly turned reddish-brown, was stirred for 4 h at 40 °C. The solid was collected, washed with cold ether, and dissolved in a minimum volume of DMF (~20 mL). This solution was stirred in the air for ~12 h, the solvent was removed in vacuo, and the reddish residue was recrystallized from dichloromethane/ether. The product (1.40 g, 60%) was obtained as shiny red-brown microcrystals. Anal. Calcd for C₄₈H₆₀Fe₂N₄O₅: C, 65.18; H, 6.79; Fe, 12.64; N, 6.34. Found: C, 64.93; H, 6.87; Fe, 12.85; N, 6.23. Absorption spectrum (CH₂Cl₂): λ_{max} (ε_M) 284 (sh, 21 500), 344 (11 000), 388 (sh, 9 500) nm.

(b) [Fe(5-*t*-Busalen)]₂S (5). The procedure is the same as that for the synthesis of [Fe(salen)]₂S⁷ except for the use of ligand 2. The crude product was recrystallized from CH₂Cl₂/hexane, affording the pure compound as reddish-brown crystals in 40% yield. Anal. Calcd for C₄₈H₆₀Fe₂N₄O₄S: C, 64.02; H, 6.67; Fe, 12.42; N, 6.22; S, 3.56. Found: C, 63.24; H, 6.74; Fe, 12.47; N, 6.15; S, 3.89. Absorption spectrum (CH₂Cl₂): λ_{max} (ε_M) 302 (17 500), 320 (sh, 16 000), 372 (sh, 8 500), 450 (7 500), 496 (sh, 7 200), 536 (sh, 6 000).

(c) [Fe(3-*t*-Busaltmen)]₂O (6). To a stirred solution of 5.00 g (11.5 mmol) of H₂(3-*t*-Busaltmen) in 20 mL of methanol was added a solution of 1.86 g (11.5 mmol) of anhydrous FeCl₃ in 30 mL of methanol after filtration through a Celite bed. The reaction was stirred for ~12 h and filtered. The residue was dissolved in a minimum volume of acetone (~20 mL) and filtered. The combined filtrate was reduced in volume until solid separated. Hexane (~30 mL) was layered on top of the solution and the mixture was cooled to 0 °C. After ~12 h standing, dark reddish-purple crystals were collected, washed with hexane, and air-dried to give 1.85 g (31%) of Fe(3-*t*-Busaltmen)Cl. This compound (1.25 g, 2.38 mmol) was dissolved in 20 mL of dichloromethane and slurried with 1.12 g (4.82 mmol) of silver(I) oxide until the color changed from reddish-purple to yellow-brown. After ~12 h the reaction mixture was filtered and the volume of the filtrate reduced until solid formed. Hexane (40 mL) was layered on top of the solution. Cooling of the mixture for 12 h at 0 °C, followed by washing of the collected solid with hexane and drying in air, afforded 1.07 g (90%) of pure product as bright red crystals. Anal. Calcd for C₅₆H₇₆Fe₂N₄O₅: C, 67.49; H, 7.63; Fe, 11.22; N, 5.62. Found: C, 66.91; H, 7.86; Fe, 11.33; N, 5.60. Absorption spectrum (CH₂Cl₂): λ_{max} (ε_M) 290 (sh, 21 000), 340 (sh, 12 300), 380 (sh, 10 200).

(d) [Fe(3-*t*-Busaltmen)]₂S (7). To a stirred solution of 0.60 g (1.12 mmol) of Fe(3-*t*-Busaltmen)Cl in 15 mL of acetonitrile was added 0.19 g (1.17 mmol) of Et₃N(SH). The color of the solution immediately darkened. The reaction mixture was stirred for ~16 h, and the reddish-brown solid was collected, washed with acetonitrile, and dried in vacuo. Recrystallization of this material from 1:1 v/v acetone/hexane gave 0.27 g (47%) of pure product as dark block-like crystals. Anal. Calcd for C₅₆H₇₆Fe₂N₄O₄S: C, 66.42; H, 7.51; Fe, 11.04; N, 5.54; S, 3.16. Found: C, 66.13; H, 8.15; Fe, 11.01; N, 5.36; S, 2.97. Absorption spectrum (CH₂Cl₂): λ_{max} (ε_M) 308 (14 200), 370 (11 000), 466 (sh, 6 800), 540 (sh, 4 200). This compound was also prepared in good yield by the method for 5.

Collection and Reduction of X-ray Data. Suitable crystals of [Fe(3-*t*-Busaltmen)]₂O and [Fe(3-*t*-Busaltmen)]₂S were grown from solutions of acetonitrile/dichloromethane and acetone/hexane, respectively, and were mounted under dinitrogen in glass capillaries. Data were collected at room temperature on a Nicolet P3F four-circle automated diffractometer with use of graphite-monochromatized Mo Kα radiation. Cell dimensions were obtained by least-squares treatment of 21–22 machine-centered reflections in the 20 ≤ 2θ ≤ 25° range. The data collection and crystal parameters are summarized in Table I. Three check reflections, monitored every 123 reflections, exhibited no significant intensity decay over the course of the two data collections. The data were processed with the program XTAPE of the SHELXTL program package (Nicolet XRD Corporation, Madison, WI), and empirical absorption corrections were applied (PSICOR). From 8915 merged reflections of the oxo compound, R_{merge} = 1.81 (5)%; with 8136 merged reflections R_{merge} = 2.54 (6)% for the sulfido compound. Monoclinic space group P2₁/a (no. 14) was uniquely established for both compounds by systematic absences. Successful solution and refinement of the structures confirmed this space group.

Solution and Refinement of the Structures. Minimally, heavy atom positions were determined in both compounds by direct methods (MULTAN) with random groups. All the remaining non-hydrogen atoms were located by Fourier maps. Atom scattering factors were taken from the tabulation of Cromer and Waber.³¹ Isotropic least-squares refinement (CRYSTALS) of all non-hydrogen atoms converged at R = 9.4% (oxo) and

Table I. Summary of Crystal Data, Intensity Collections, and Structure Refinement Parameters

	[Fe(3- <i>t</i> -Busaltmen)] ₂ O	[Fe(3- <i>t</i> -Busaltmen)] ₂ S
formula	C ₅₆ H ₇₆ Fe ₂ O ₅ N ₄	C ₅₆ H ₇₆ Fe ₂ O ₄ N ₄ S ₁
mol wt	996.93	1013.00
a (Å)	20.395 (3)	20.931 (8)
b (Å)	11.864 (3)	11.884 (6)
c (Å)	24.311 (4)	24.229 (7)
β (deg)	114.61 (1)	114.34 (2)
crystal system	monoclinic	monoclinic
V (Å ³)	5348 (2)	5491 (4)
Z	4	4
d _{calcd} (g/cm ³)	1.23	1.23
d _{obsd} (g/cm ³)	1.22 ^a	1.21 ^a
space group	P2 ₁ /a	P2 ₁ /a
cryst dimns (mm)	0.70 × 0.30 × 0.25	0.60 × 0.30 × 0.20
radiation	Mo Kα (λ = 0.71069)	Mo Kα (λ = 0.71069)
abs coeff, μ, (cm ⁻¹)	5.9	6.1
scan speed (deg/min)	2.0–29.3 (ω scan)	2.0–29.3 (ω scan)
scan range (deg)	0.6	0.6
bkgd/scan time ratio	0.25	0.25
2θ limits	3° ≤ 2θ ≤ 49°	3° ≤ 2θ ≤ 47°
data collected	9945 (+h,+k,±l)	9135 (+h,+k,±l)
R _{merge} ^b (%)	1.81 (5)	2.54 (6)
unique data (F _o ² > 2.5σ(F _o ²))	4471	3642
no. of variables	605	485
R (R _w) ^c (%)	5.80 (5.26) ^d	6.48 (5.87) ^d

^a Determined by the neutral buoyancy in CCl₄/heptane. ^b R_{merge} = [Σ(N_iΣ_j|(F_i - F_j)/Σ(N_iΣ_jF_j))] where N_i is the number of equivalent reflections merged to give the mean, F_i, F_j is any one member of this set, and the calculations are done on a scale of F_o². ^c R = Σ||F_o - |F_c||/Σ|F_o|; R_w = [Σw(|F_o|² - |F_c|²)/Σw|F_o|²]^{1/2}. ^d Weighting scheme for least-squares refinement: w = (F_o/P(1))², F_o ≤ P(1); w = (P(1)/F_o)², F_o > P(1), where P(1) = F(min(|F_o|² - |F_c|²)) = 25.0 (20.0) 0(S).

9.9% (sulfido). With the oxo compound, all non-hydrogen atoms were refined anisotropically; phenyl carbon atoms were refined as semirigid bodies. Owing to a less than optimal data set for the sulfido compound, only the non-phenyl, non-hydrogen atoms were described anisotropically. In the last stages of refinement, hydrogen atoms with thermal parameters set at 1.2× that of the bonded carbon atom and fixed C–H distance of 0.96 Å were included. The final difference Fourier maps of both compounds showed a single peak of ~0.9 e⁻/Å³ at the origin and no other peaks >0.4 e⁻/Å³. Unique data used in the refinements and final R factors are given in Table I. Positional parameters are listed in Tables II and III.³²

Other Physical Measurements. All measurements were made under anaerobic conditions with freshly dried solvents. Absorption spectra were recorded on a Cary Model 219 spectrophotometer and ¹H NMR spectra on a Bruker AM-300 or AM-500 spectrometer with Me₄Si as the internal standard. Electrochemical measurements were made at room temperature with standard PAR instrumentation, a glassy carbon working electrode, a SCE reference electrode, and 0.1 M (n-Bu₄N)(ClO₄) supporting electrolyte. Magnetic susceptibility determinations of solids were performed on finely ground samples with a SHE 905 SQUID magnetometer operating between 6 and 300 K. Solution measurements were made by the usual NMR method³³ with Me₄Si as the reference. Dichloromethane solution densities were corrected for changes in temperature by use of the temperature dependence of the solvent density.³⁴ Solvent susceptibility was a literature value.³⁵ The diamagnetic correction for salen was taken as the measured value for H₂salen of -154.8 × 10⁻⁶ cgsu/mol,³⁶ leading to total diamagnetic corrections of -626 × 10⁻⁶ and -652 × 10⁻⁶ cgsu/mol for [Fe(3-*t*-Busaltmen)]₂O and [Fe(3-*t*-Busaltmen)]₂S, respectively, when ligand substituent contributions calculated from Pascal's constants³⁷ are included. Magnetic susceptibility data for solid samples are tabulated.³²

(32) See paragraph at the end of this article regarding supplementary material.

(33) (a) Evans, D. F. *J. Chem. Soc.* **1959**, 2003. (b) Live, D. H.; Chan, S. I. *Anal. Chem.* **1970**, 42, 79.

(34) *TRC Thermodynamic Tables*; Thermodynamics Research Center, The Texas A&M University System, College Station, TX, 1985; pp d-7240 to d-7241. The density data were fit to a four-term polynomial in T(K): d(g/cm³) = (2.007 × 10⁻⁹)T³ + (2.061 × 10⁻⁷)T² - (2.195 × 10⁻³)T + 1.907 (T = 183–323 K).

(35) Gerger, W.; Mayer, U.; Gutmann, V. *Monatsh. Chem.* **1977**, 108, 417.

(36) Belova, V. I.; Syrkin, Ya. K. *Bull. Acad. Sci. USSR (Div. Chem. Sci.)* **1961**, 1778.

(37) O'Connor, C. J. *Prog. Inorg. Chem.* **1982**, 29, 203.

(31) Cromer, D. T.; Waber, J. T. *International Critical Tables for X-ray Crystallography*; Kynoch Press: Birmingham, England, 1974.

Table II. Positional Parameters ($\times 10^4$) for $[\text{Fe}(3-t\text{Busaltmen})]_2\text{O}$

atom	x/a	y/b	z/c
Fe(1)	3885.3 (5)	901.9 (7)	2505.8 (4)
Fe(2)	2144.9 (4)	1335.3 (7)	2469.6 (4)
O(1)	3032 (2)	1184 (4)	2517 (2)
O(a)	3853 (2)	1044 (4)	1706 (2)
O(b)	3972 (2)	-712 (3)	2497 (2)
O(c)	1637 (2)	-33 (4)	2447 (2)
O(d)	2276 (2)	1670 (4)	3284 (2)
N(a)	4407 (2)	2501 (4)	2671 (2)
N(b)	4679 (2)	790 (5)	3409 (2)
N(c)	1513 (3)	1411 (5)	1530 (2)
N(d)	1837 (3)	3069 (4)	2303 (2)
C(1a)	4115 (3)	2960 (5)	1624 (3)
C(2a)	3852 (3)	1906 (6)	1364 (3)
C(3a)	3614 (3)	1739 (6)	737 (3)
C(4a)	3652 (4)	2658 (7)	392 (3)
C(5a)	3909 (4)	3698 (7)	646 (3)
C(6a)	4142 (3)	3854 (6)	1258 (3)
C(7a)	4400 (4)	3176 (6)	2257 (3)
C(8a)	4728 (3)	2829 (6)	3319 (3)
C(9a)	4116 (4)	3068 (6)	3491 (3)
C(10a)	5215 (4)	3872 (6)	3455 (3)
C(11a)	3346 (5)	579 (8)	459 (3)
C(12a)	3080 (7)	626 (10)	-242 (4)
C(13a)	2726 (5)	165 (9)	585 (4)
C(14a)	3963 (6)	-269 (8)	698 (4)
C(1b)	4407 (3)	-1165 (5)	3530 (3)
C(2b)	4052 (3)	-1456 (5)	2915 (3)
C(3b)	3797 (3)	-2571 (5)	2754 (3)
C(4b)	3905 (3)	-3326 (5)	3215 (3)
C(5b)	4252 (4)	-3051 (6)	3822 (3)
C(6b)	4508 (3)	-1972 (6)	3976 (3)
C(7b)	4743 (3)	-100 (6)	3729 (3)
C(8b)	5166 (3)	1778 (6)	3658 (3)
C(9b)	5819 (4)	1553 (6)	3505 (4)
C(10b)	5432 (4)	1893 (7)	4344 (3)
C(11b)	3417 (4)	-2924 (6)	2089 (3)
C(12b)	2718 (4)	-2228 (7)	1786 (3)
C(13b)	3205 (5)	-4164 (7)	2019 (4)
C(14b)	3911 (4)	-2746 (7)	1767 (3)
C(1c)	1054 (3)	-518 (5)	1413 (3)
C(2c)	1273 (3)	-763 (5)	2032 (3)
C(3c)	1073 (3)	-1820 (5)	2193 (3)
C(4c)	679 (3)	-2561 (5)	1731 (3)
C(5c)	474 (3)	-2319 (6)	1121 (3)
C(6c)	663 (3)	-1296 (6)	962 (3)
C(7c)	1157 (4)	578 (6)	1196 (3)
C(8c)	1505 (4)	2544 (6)	1257 (3)
C(9c)	942 (4)	2643 (7)	606 (4)
C(10c)	2249 (4)	2767 (7)	1294 (4)
C(11c)	1291 (4)	-2125 (5)	2859 (3)
C(12c)	949 (4)	-1284 (6)	3140 (3)
C(13c)	1008 (4)	-3314 (6)	2924 (4)
C(14c)	2110 (4)	-2121 (7)	3206 (4)
C(1d)	2462 (3)	3634 (5)	3352 (3)
C(2d)	2540 (3)	2563 (5)	3621 (3)
C(3d)	2896 (3)	2461 (5)	4256 (3)
C(4d)	3178 (3)	3427 (6)	4591 (3)
C(5d)	3107 (4)	4485 (6)	4324 (3)
C(6d)	2740 (3)	4593 (6)	3705 (3)
C(7d)	2063 (3)	3816 (5)	2719 (3)
C(8d)	1332 (4)	3350 (6)	1679 (3)
C(9d)	582 (4)	3125 (8)	1669 (4)
C(10d)	1357 (5)	4594 (7)	1506 (4)
C(11d)	2980 (3)	1301 (7)	4557 (3)
C(12d)	2236 (4)	770 (7)	4387 (3)
C(13d)	3445 (4)	532 (6)	4369 (3)
C(14d)	3331 (4)	1382 (8)	5260 (3)

Table III. Positional Parameters ($\times 10^4$) for $[\text{Fe}(3-t\text{Busaltmen})]_2\text{S}$

atom	x/a	y/b	z/c
Fe(1)	6018.1 (6)	762 (1)	2479.7 (5)
Fe(2)	8045.8 (7)	1354 (1)	2535.6 (6)
S(1)	7031 (1)	876 (3)	2463 (1)
O(a)	6091 (3)	946 (5)	3282 (2)
O(b)	5909 (3)	-839 (5)	2492 (2)
O(c)	8579 (3)	36 (5)	2552 (2)
O(d)	7861 (3)	1720 (5)	1716 (2)
N(a)	5580 (3)	2400 (5)	2318 (3)
N(b)	5268 (3)	691 (7)	1577 (3)
N(c)	8638 (4)	1438 (7)	3484 (3)
N(d)	8240 (3)	3097 (6)	2707 (3)
C(1a)	5908 (3)	2880 (6)	3380 (4)
C(2a)	6149 (3)	1813 (6)	3627 (3)
C(3a)	6420 (3)	1681 (6)	4261 (3)
C(4a)	6421 (4)	2608 (7)	4612 (4)
C(5a)	6170 (4)	3658 (8)	4368 (4)
C(6a)	5915 (4)	3803 (7)	3743 (4)
C(7a)	5610 (4)	3096 (7)	2736 (4)
C(8a)	5240 (4)	2736 (7)	1665 (4)
C(9a)	4796 (5)	3804 (7)	1559 (4)
C(10a)	5842 (5)	2978 (8)	1472 (4)
C(11a)	6669 (6)	534 (9)	4546 (4)
C(12a)	7257 (6)	87 (11)	4388 (5)
C(13a)	6076 (6)	-323 (9)	4352 (5)
C(14a)	6990 (8)	580 (12)	5251 (5)
C(1b)	5526 (3)	-1250 (7)	1452 (3)
C(2b)	5874 (3)	-1555 (6)	2066 (3)
C(3b)	6150 (4)	-2652 (6)	2219 (4)
C(4b)	6075 (4)	-3410 (7)	1766 (4)
C(5b)	5722 (4)	-3117 (7)	1157 (4)
C(6b)	5450 (4)	-2044 (7)	998 (4)
C(7b)	5192 (4)	-188 (8)	1251 (4)
C(8b)	4809 (4)	1690 (8)	1341 (4)
C(9b)	4176 (4)	1510 (8)	1493 (5)
C(10b)	4552 (5)	1796 (8)	647 (4)
C(11b)	6547 (5)	-3006 (8)	2879 (5)
C(12b)	7203 (5)	-2270 (10)	3180 (5)
C(13b)	6789 (6)	-4239 (9)	2942 (5)
C(14b)	6096 (6)	-2870 (9)	3235 (5)
C(1c)	9053 (4)	-499 (7)	3574 (4)
C(2c)	8862 (3)	-742 (7)	2957 (3)
C(3c)	9008 (3)	-1811 (6)	2789 (3)
C(4c)	9346 (4)	-2591 (7)	3245 (4)
C(5c)	9544 (4)	-2369 (8)	3855 (4)
C(6c)	9388 (4)	-1319 (8)	4021 (4)
C(7c)	8961 (5)	605 (9)	3795 (4)
C(8c)	8618 (5)	2535 (8)	3761 (4)
C(9c)	9181 (6)	2648 (10)	4418 (4)
C(10c)	7881 (6)	2679 (9)	3750 (5)
C(11c)	8767 (5)	-2140 (7)	2124 (4)
C(12c)	7971 (5)	-2043 (9)	1801 (4)
C(13c)	8982 (6)	-3339 (8)	2047 (5)
C(14c)	9109 (5)	-1352 (8)	1819 (5)
C(1d)	7562 (3)	3647 (6)	1658 (3)
C(2d)	7528 (4)	2593 (6)	1389 (3)
C(3d)	7149 (3)	2460 (6)	761 (3)
C(4d)	6818 (4)	3408 (6)	428 (4)
C(5d)	6857 (4)	4457 (7)	697 (4)
C(6d)	7237 (4)	4588 (7)	1311 (4)
C(7d)	7970 (4)	3838 (7)	2286 (4)
C(8d)	8725 (4)	3422 (7)	3332 (4)
C(9d)	8630 (6)	4606 (8)	3503 (5)
C(10d)	9466 (5)	3299 (10)	3348 (5)
C(11d)	7087 (5)	1324 (9)	449 (4)
C(12d)	6688 (6)	1383 (10)	-242 (4)
C(13d)	6683 (5)	478 (9)	681 (4)
C(14d)	7812 (5)	837 (10)	585 (4)

Molecular Orbital Calculations. Orbital exponents and H_{ii} values used in the extended Hückel calculations were taken from the literature.³⁸ Computational details followed those described by Ammeter et al.³⁹

(38) (a) Tatsumi, K.; Hoffmann, R. *J. Am. Chem. Soc.* **1981**, *103*, 3328. (b) Sung, S.-S.; Glidewell, C.; Butler, A. R.; Hoffmann, R. *Inorg. Chem.* **1985**, *24*, 3856.

(39) Ammeter, J. H.; Bürgi, H.-B.; Thibeault, J. C.; Hoffmann, R. *J. Am. Chem. Soc.* **1978**, *100*, 3686.

Results and Discussion

Complexes of immediate pertinence to the present investigation are 4–11. Structures of $[\text{Fe}(\text{acen})]_2\text{X}^8$ are schematically illustrated. Complexes 4 and 5 are solubilized versions of 8 and 9, useful for the examination of solution properties without significantly altering the structures of the unsubstituted species. Complexes 6 and 7 are adequately soluble for solution work and are substituted with the intention of changing the bridge angles

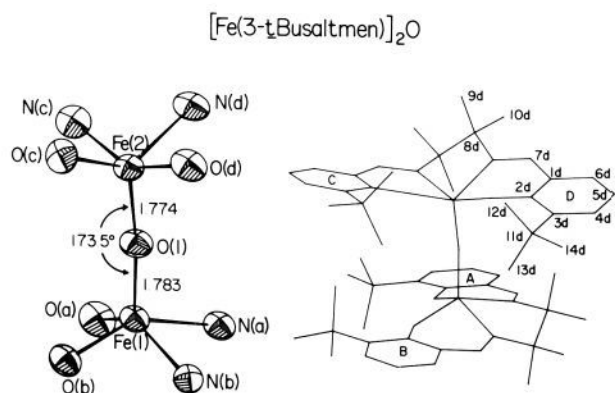
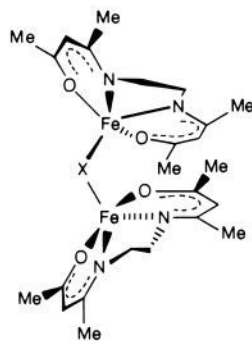
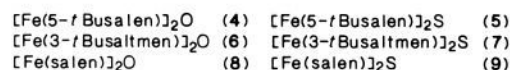


Figure 1. Structure of $[\text{Fe}(3\text{-}t\text{Busaltmen})]_2\text{O}$: right, entire structure and atom labeling scheme for ring D; left, coordination unit with 50% thermal ellipsoids and atom labeling. In this and the following figure, ligand portions A–C have a labeling scheme analogous to portion D.

while largely unaffected the geometrical and electronic features of the half-dimers.



$[\text{Fe}(\text{acen})]_2\text{O}$ (10) $[\text{Fe}(\text{acen})]_2\text{S}$ (11)

Angles of unsupported Fe–O–Fe bridges in Fe(III) complexes fall in the range 139–180°. ^{1,8,19,40,41} The lower limit of 139.1 (9)° is found with the crystalline solvate compound $[\text{Fe}(\text{salen})]_2\text{O}\cdot 2\text{py}$.²⁰ The values of 121.8 (1)° in $[\text{Fe}(\text{salen})]_2\text{S}$ ⁷ and 120.8 (1) in $[\text{Fe}(\text{acen})]_2\text{S}$ ⁸ are the only angular measures of the unsupported Fe–S–Fe bridge prior to this investigation. While it is not known whether the *intrinsic* angles of the $[\text{Fe}_2\text{X}]^{4+}$ groups (X = O, S) are less than those values, it is highly probable that they represent lower limits inasmuch as any alteration of the basic acen or salen ligand structure (excluding such obvious circumstances as Me/H substitution or the introduction of an ethylenic bridge in acen) potentially could lead to increased steric repulsion between half-dimers. Although the foregoing range of Fe–O–Fe angles suggests a “softness” to bending, this property has never been examined in cases where the essential ligand structure remains constant and half-dimer nonbonded repulsions were adjusted by ligand substitution. Scrutiny of space-filling models and calculations of nonbonded interactions (*vide infra*) suggested that, in the known conformation of $[\text{Fe}(\text{salen})]_2\text{O}$, substitution at the 3-position of the salicylaldiminato chelate ring *and* at the methylene carbon atoms would bring the half-dimers into van der Waals contact unless the bridge angle was appreciably enlarged. This angle would be driven to open in order to attenuate these repulsions. Appropriate substitution at both of these sites appeared to offer a feasible means to increase bridge angles. This matter has been pursued by use of the saltmen ligand system 3, a variation

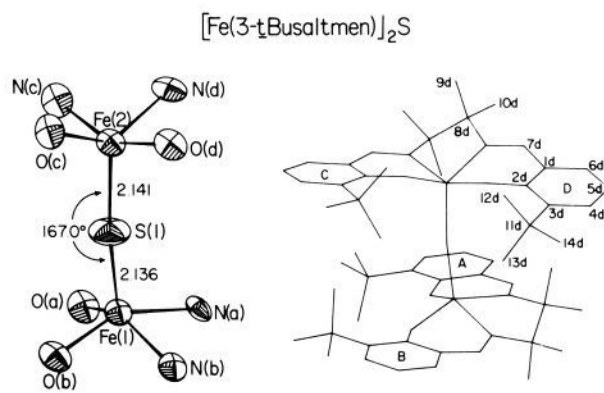


Figure 2. Structure of $[\text{Fe}(3\text{-}t\text{Busaltmen})]_2\text{S}$: right, entire structure and atom labeling scheme for ring D; left, coordination unit with 50% thermal ellipsoids and atom labeling.

Table IV. Selected Interatomic Distances (Å) and Angles (deg) for $[\text{Fe}(3\text{-}t\text{Busaltmen})]_2\text{X}$ (X = O, S)

distance/angle	X = O	X = S
Fe(1)–X(1)	1.783 (4)	2.141 (3)
Fe(2)–X(1)	1.774 (4)	2.135 (3)
Fe(1)–O(a)	1.926 (4)	1.899 (5)
Fe(1)–O(b)	1.924 (4)	1.918 (6)
Fe(1)–N(a)	2.130 (5)	2.119 (6)
Fe(1)–N(b)	2.121 (5)	2.103 (7)
Fe(2)–O(c)	1.915 (4)	1.914 (6)
Fe(2)–O(d)	1.925 (4)	1.909 (6)
Fe(2)–N(c)	2.105 (5)	2.117 (7)
Fe(2)–N(d)	2.139 (5)	2.119 (7)
Fe(1)–X(1)–Fe(2)	173.45 (27)	167.01 (18)
O(a)–Fe(1)–O(b)	92.34 (19)	93.35 (25)
O(a)–Fe(1)–N(a)	85.24 (19)	85.95 (26)
O(a)–Fe(1)–N(b)	137.81 (18)	141.17 (25)
O(b)–Fe(1)–N(b)	85.10 (19)	86.19 (28)
O(b)–Fe(1)–N(a)	147.94 (19)	150.37 (24)
N(a)–Fe(1)–N(b)	75.78 (20)	76.32 (29)
O(c)–Fe(2)–O(d)	92.63 (18)	94.28 (24)
O(c)–Fe(2)–N(c)	85.75 (19)	86.58 (27)
O(d)–Fe(2)–N(d)	84.32 (19)	85.47 (26)
N(c)–Fe(2)–N(d)	75.81 (22)	76.26 (30)
O(d)–Fe(2)–N(c)	150.10 (19)	153.54 (26)
O(c)–Fe(2)–N(d)	134.22 (18)	137.11 (26)

of the salen workhorse **1** in which the two-carbon bridge carries four methyl groups. The crystalline compounds **6** and **7** were synthesized by known routes and subjected to a variety of investigations in the solid and solution states. As will be seen, the desired structural result was achieved for both $[\text{Fe}_2\text{X}]^{4+}$ groups in these complexes.

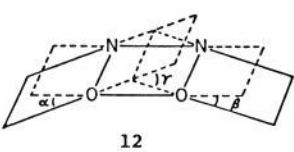
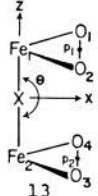
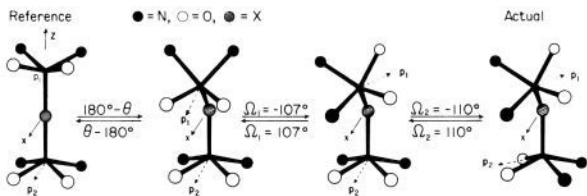
Structures of Oxo- and Sulfido-Bridged complexes. $[\text{Fe}(3\text{-}t\text{Busaltmen})]_2\text{O}$ and $[\text{Fe}(3\text{-}t\text{Busaltmen})]_2\text{S}$ crystallize in monoclinic space group $P2_1/a$ in practically isomeric unit cells, a behavior no doubt associated with their closely similar molecular conformations. There is no imposed symmetry. Their structures are presented in Figures 1 and 2, which include a schematic rendering of the entire molecule and a detailed view of the metal coordination units. Selected interatomic distances and angles are collected in Table IV. Metric features of the $\text{Fe}(\text{salen})$ portions are unexceptional and are not considered further. In particular, angles and distances in the FeO_2N_2 coordination units accord well with previous investigations in the salen series.^{20–22} Stereoviews of both structures are available.³²

(a) Bridge Units. Bridge structural data for the pairs **6/7**, **8/9**, and **10/11** of oxo- and sulfido-bridged complexes are collected in Table V, in which **12** and **13** illustrate angular parameters useful in describing ligand structure and relative orientation of half-dimers.

The half-dimers have small structural differences, but all adopt the familiar “umbrella-shaped” ligand configuration, with unexceptional values of the dihedral angle parameters α , β , γ ¹⁹ (cf.

(40) Drew, M. G. B.; McKee, V.; Nelson, S. M. *J. Chem. Soc., Dalton Trans.* **1978**, 80.

(41) Thich, J. A.; Toby, B. H.; Powers, D. A.; Potenza, J. A.; Schugar, H. *J. Inorg. Chem.* **1981**, *20*, 3314.

Table V. Bridge and Conformational Features of $\mu\text{-X}$ Complexes (X = O, S)




complex	distance, Å			angle, deg							ref
	Fe-X	Fe...Fe	δ	θ	α	β	γ	Ω_1	Ω_2		
$[\text{Fe}(\text{salen})]_2\text{O}^f$	1.78 (1) ^a	3.391	0.581	144.6 (6)	4.5	14.3	10.7	-107.5	-110.7	22	
$[\text{Fe}(3\text{-}t\text{Busaltmen})]_2\text{O}$	1.779 (5) ^a	3.551	0.572	173.4 (3)	8.56	13.5	15.9	-9.09	-92.8	d	
			0.621 ^b								
$[\text{Fe}(\text{acen})]_2\text{O}^e$	1.775 (13)	3.433 (3)	0.607	150.7 (13)	19.8	7.67	27.3	+117.7	+114.7	8	
			0.564								
$[\text{Fe}(\text{salen})]_2\text{S}$	2.150 (2)	3.792	0.625	121.8 (1)	11.5	17.2	26.5	-110.8	-120.2	7	
			0.591								
$[\text{Fe}(3\text{-}t\text{Busaltmen})]_2\text{S}$	2.138 (3) ^a	4.249	0.569 ^c	167.0 (2)	5.80	10.7	13.8	+152.6	+108.4	d	
			0.566 ^b								
$[\text{Fe}(\text{acen})]_2\text{S}^e$	2.207 (4) ^a	3.838 (2)	0.584	120.8 (1)	22.2	22.4	44.5	-119.9	-119.5	8	
			0.584								

^a Mean value. ^b Fe(1). ^c Fe(2). ^d This work. ^e Data recalculated from positional parameters in ref 8. ^f $[\text{Fe}(\text{salen})]_2\text{O}\cdot 2\text{py}$: $[\theta, \Omega_1, \Omega_2] = [139.1(9), -103.2, -105.9]$; ²⁰ $[\text{Fe}(\text{salen})]_2\text{O}\cdot \text{CH}_2\text{Cl}_2$: $[\theta, \Omega_1, \Omega_2] = [142.4(5), -77.6, -115.5]$.²¹

12). The Fe atoms are displaced from the coordination plane toward bridge atom X by $\delta \approx 0.6$ Å; there is no correlation between γ and the displacement δ . In comparison with the unsubstituted salen complexes, all structural aspects of $[\text{Fe}(3\text{-}t\text{Busaltmen})]_2\text{O}$ and $[\text{Fe}(3\text{-}t\text{Busaltmen})]_2\text{S}$ are normal except for the bridge angles θ .

It is immediately evident that ligand substitution has caused large increases in bridge angles: 28.8° for the oxo bridge in 6 and 45.2° for the sulfido bridge in 7. As the Fe-O-Fe angle approaches linearity, the Fe-O distance remains essentially unchanged at 1.78 Å and the Fe atom displacement from the coordination plane increases by about 0.04 Å. When the Fe-S-Fe angle is opened, the unsymmetrical bridge in $[\text{Fe}(\text{salen})]_2\text{S}$ disappears and the new bridge very closely approaches C_{2v} symmetry, as found with the oxo bridges. However, the Fe-S distances and δ both decrease, by 0.01–0.04 and 0.03–0.05 Å, respectively. Iron atom displacements from mean planes are difficult to interpret because of accompanying relative changes in oxygen and nitrogen atom positions, which define these planes. Nonetheless, the large displacement in 6 seemingly can only be due to steric tension between half-dimers, leading to a locked conformation (vide infra). In contrast, the Fe atom in 7 tends to move toward the plane, an effect most likely due to the longer bond distance to the bridge atom. All metric features of oxo or sulfido bridges differ by relatively small amounts except for the bridge angle. Because of this, significant differences in properties of the same bridge group at dissimilar bridge angles, as manifested by salen and saltmen complexes, are attributed mainly to differences in this angle.

(b) **Conformational Aspects.** Specification of the relative orientations of two half-dimers of the $\text{Fe}(\text{salen})$ type (i.e., local twofold symmetry) is a problem of modest complexity. It has not been previously addressed and has been solved here to provide a means of structural description of such molecules and for use in electronic structural calculations (vide infra). One method affording an unambiguous description utilizes 13 and is shown as eq 1 in Table V. Define the midpoints of the O(1)–O(2) and

O(3)–O(4) vectors as p_1 and p_2 , respectively. Place the molecule in the C_{2v} reference configuration, in which $\theta = 180^\circ$ and the vectors Fe(1)– p_1 and Fe(2)– p_2 lie in the same (mean) plane. In this arrangement, the two half-dimers eclipse each other or approach this condition as closely as the actual structure will permit. Define a fixed coordinate system at the bridge atom such that the z-axis is along the Fe–X vectors and the +x-axis lies in the (mean) plane of the vectors Fe(1)– p_1 and Fe(2)– p_2 . A positive value of the bridge angle θ corresponds to a bend of the half-dimers in the xz plane toward the +x-axis. Lastly, define the dihedral angles $\Omega_1 = p_1\text{Fe}(1)\text{XFe}(2)$ and $\Omega_2 = p_2\text{Fe}(2)\text{XFe}(1)$, positive values of which refer to clockwise rotations when viewed down the Fe(1)–X and Fe(2)–X directions, respectively. Application of the operations $+(180^\circ - \theta) + (-\Omega_1) + (-\Omega_2)$ generates the conformation $[\theta, \Omega_1, \Omega_2]$ from the reference state. Application of $+(\Omega_1) + (\Omega_2) + (-180^\circ + \theta)$ recovers the reference conformation from any other.⁴² Values of $[\theta, \Omega_1, \Omega_2]$ for the preceding three pairs of compounds, and for two solvates of $[\text{Fe}(\text{salen})]_2\text{O}$, are set out in Table V. The signs of Ω_1 and Ω_2 , which are the same for any particular configuration, depend on molecular chirality. All molecules in Table V crystallize in centrosymmetric space groups.

The conformational angles $\Omega_{1,2}$ vary over a substantial range and, in conjunction with nonlinear bridges, are difficult to rationalize on intuitive grounds. It is apparent that some of these angles with the same ligand system can be affected by the exigencies of individual crystal packing. Thus in the series $[\text{Fe}(\text{salen})]_2\text{O}$, $[\text{Fe}(\text{salen})]_2\text{O}\cdot 2\text{py}$, and $[\text{Fe}(\text{salen})]_2\text{O}\cdot \text{CH}_2\text{Cl}_2$, angles of the first two complexes are quite similar, but those of the third are clearly different. Certain seeming regularities are observed, however. The conformations of $[\text{Fe}(\text{salen})]_2\text{O}$ and $[\text{Fe}(\text{salen})]_2\text{S}$ are clearly similar, as are those of enantiomerically related $[\text{Fe}$

(42) Note that only two angular operations are necessary to pass from the actual to the reference conformation. However, the converse is not always true; to ensure a commutative relationship in both directions, three operations are defined.

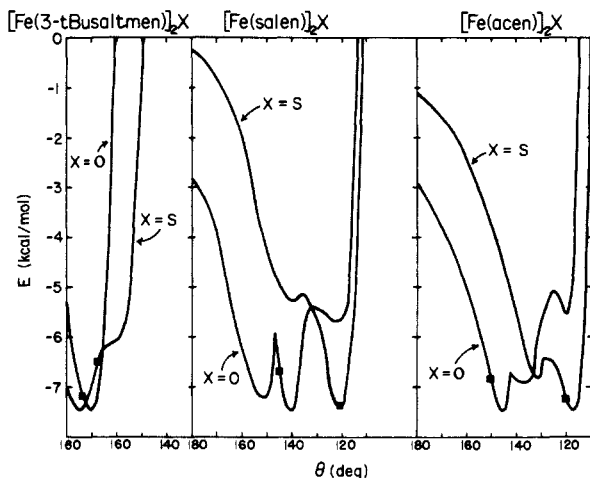


Figure 3. Relative van der Waals energies (kcal/mol) of the indicated pairs of complexes ($X = O, S$) as dependent on bridge angle θ . Observed conformations in the crystalline state are indicated (■).

(acen) $_2O$ and [Fe(acen) $_2S$, despite the large differences in bridge angles. Despite the departures in $\Omega_{1,2}$ angles, the conformations of [Fe(3-*t*Busaltmen) $_2X$ are actually very similar.⁴³ Lastly, all values of θ are positive.

The conformations of the parts of complexes 6/7, 8/9, and 10/11 have been investigated by using an approximate, nonbonded repulsion model based on the van der Waals potential^{2,44} in which r is an interatomic distance and the remaining terms are interaction coefficients between atom pairs. Calculations were performed

$$V(r) = \sum [a \exp(-br)/r^d - cr^{-6}] \quad (2)$$

by means of the program MODEL from the ChemGraf suite of programs.⁴⁵ Iron atoms were (arbitrarily) replaced with oxygen atoms; coulombic interactions were omitted.

Results of the van der Waals calculations are plotted in Figure 3. These curves were obtained by determining the minimum energy-conformation at each value of θ by searching over all $[\Omega_1, \Omega_2]$ conformations at fixed bridge angle; i.e., each point on a curve corresponds to a potential energy minimum at specified θ and variable $\Omega_{1,2}$ angles. Because of this and nonperiodic repulsive interactions between half-dimers, the potential energy curves exhibit sharp points and irregular patterns. The following principal aspects emerge from the calculations. (i) No stable conformations with $\theta = 180^\circ$ are predicted, and no linear bridges have been found. (ii) Oxo complexes are stabilized at larger θ values than are sulfido complexes for 8/9 and 10/11, as observed; for 6/7 the prediction is reversed (and contrary to experiment) but the energy minima are separated by less than 5° . (iii) Substitution at the 3-ring and bridge positions (ligand 3) affords for 6/7 a much narrower range of low-energy conformations than for other complexes and suggests no stable conformations with $\theta \lesssim 165^\circ$; i.e., ligand-ligand repulsions override preferred bridge angle differences. (iv) Similar minimum energy conformations in θ are predicted for acen and salen complexes with the same bridge atom, as observed. (v) Values of $[\theta, \Omega_1, \Omega_2]$ for energy-

(43) This situation arises because of the unusual position of the oxo bridge atom in 6. Note that the $\Omega_{1,2}$ angles depend on position of bridge atom X. In all other compounds in Table V, the bridge atom is placed, upon bending to $\theta < 180^\circ$, into the least congested area between half-dimers. This area lies between the Fe atoms on the bisector of the dihedral angle formed by p_1 and p_2 when viewing down the Fe-Fe vector. In 6, the bridge atom is nearly 180° from the "usual" position; owing to the near-linearity of the bridge, it is possible that this and the usual position are of nearly equal energy.

(44) (a) Coiro, V. M.; Giglio, E.; Quagliata, C. *Acta Crystallogr.* 1972, B28, 3601. Pavel, N. V.; Quagliata, C.; Scarcelli, N. *Z. Kristallogr.* 1976, 144, 64. (c) Del Re, G.; Gavuzzo, E.; Giglio, E.; Lej, F.; Mazza, F.; Zappia, V. *Acta Crystallogr.* 1977, B33, 3289.

(45) "ChemGraf", created by E. K. Davies; Chemical Crystallography Laboratory, Oxford University, 1985; developed and distributed by Chemical Design Ltd., Oxford, England.

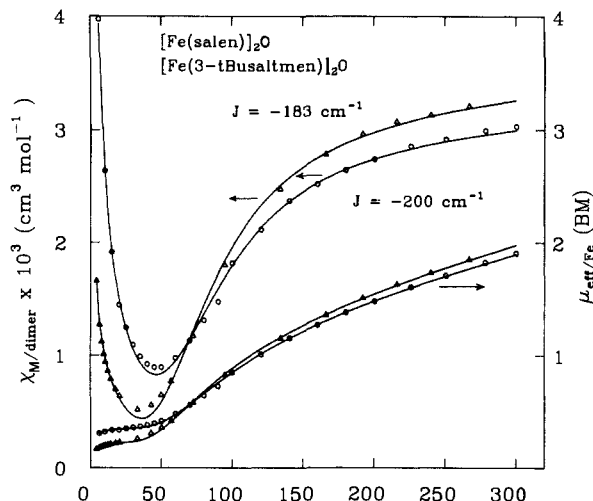


Figure 4. Temperature dependencies of the molar magnetic susceptibilities and magnetic moments $\mu(\mu_B) = 2.829[\chi^M T]^{1/2}$ (lower curves) for [Fe(salen) $_2O$ and [Fe(3-*t*Busaltmen) $_2O$. The solid lines are theoretical fits using the parameter sets in Table VI.

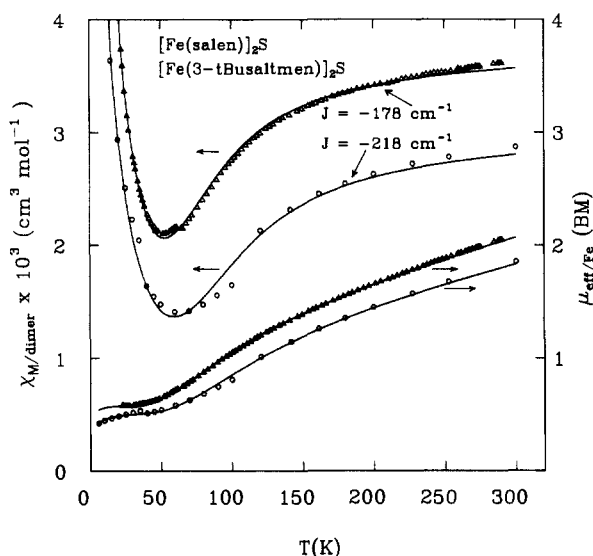


Figure 5. Temperature dependencies of the molar magnetic susceptibilities and magnetic moments $\mu(\mu_B) = 2.829[\chi^M T]^{1/2}$ (lower curves) for [Fe(salen) $_2S$ and [Fe(3-*t*Busaltmen) $_2S$. The solid lines are theoretical fits using the parameter sets in Table VI.

minimized conformations are generally in very good agreement with the data from crystal structures in Table V. One clear effect is that all observed conformations are disposed so as to reduce repulsive interactions between ethylene bridges.

Despite its simplified nature, the van der Waals model based on the potential 2 is quite effective in rationalizing minimum energy conformations, which are designated in θ in Figure 3. We conclude that *the conformations of complexes 6-11 are largely determined by nonbonded repulsions amongst half-dimers and bridge atoms*. It is, therefore, not surprising that in two crystalline environments the conformation of [Fe(salen) $_2O$ is nearly constant. Evidently in the third crystalline form, the dichloromethane solvate molecule packs so as to perturb the otherwise favored conformation. Further, repulsive forces are capable of deforming the normally less obtuse angle at sulfur to very near that value (173°) calculated for the minimum energy structure of [Fe(3-*t*Busaltmen) $_2S$.

Magnetism. The antiferromagnetism of [Fe(salen) $_2O$ ²⁶ and [Fe(salen) $_2S$ ⁷ is well established and is describable by eq 3, developed under the usual spin Hamiltonian $\mathcal{H} = -JS_1 \cdot S_2$. The fraction of paramagnetic impurity is given by ρ and was treated as high-spin Fe(III); other symbols have their usual meanings.

Table VI. Parameters for Magnetic Susceptibility Data^{a,c}

J (cm ⁻¹)	$10^3 \rho$	g	Φ (K)	R^b
[Fe(salen)] ₂ O ^c				
-183*	3.72*	2.0023	-6.08*	5.40×10^{-4}
-181*	1.94*	2.0023*	0	6.82×10^{-3}
-184*	3.74*	2.009*	-6.15*	5.37×10^{-4}
[Fe(3- <i>t</i> -Busaltmen)] ₂ O				
-200*	7.87*	2.0023	-2.75*	4.32×10^{-4}
-197*	5.93*	2.0023*	0	4.24×10^{-3}
-203*	7.94*	2.029*	-2.85*	3.97×10^{-4}
[Fe(salen)] ₂ S ^d				
-178*	20.2*	2.0023	-1.26*	9.35×10^{-5}
-178*	19.4*	2.010*	0	1.06×10^{-4}
-184*	21.7*	2.047*	-3.39*	5.80×10^{-5}
[Fe(3- <i>t</i> -Busaltmen)] ₂ S				
-218*	16.1*	2.0023	-3.60*	1.02×10^{-3}
-207*	11.3*	2.0023*	0	1.35×10^{-2}
-228*	16.2*	2.087*	-3.73*	8.81×10^{-4}

^aDiamagnetic corrections (cgsu) used in data fitting: [Fe(salen)]₂O, -342×10^{-6} ; [Fe(salen)]₂S, -368×10^{-6} ; [Fe(3-*t*-Busaltmen)]₂O, -626×10^{-6} ; [Fe(3-*t*-Busaltmen)]₂S, -652×10^{-6} . ^b $R = \sum [\chi^{\text{M,expt}} - \chi^{\text{M,calc}}]^2 / \sum [\chi^{\text{M,expt}}]^2$. ^cExperimental susceptibilities from ref 26, where data were fit with $J = -178$ cm⁻¹. ^dExperimental susceptibilities from ref 7, where data were fit with $J = -176$ cm⁻¹. ^eParameters allowed to float in a given fit are marked with an asterisk; g values were not allowed to float below the free electron value (2.0023).

The complexes [Fe(3-*t*-Busaltmen)]₂O and [Fe(3-*t*-Busaltmen)]₂S, with their enlarged bridge angles, offer the best available cases

$$\chi^{\text{M}} = (g^2 \beta^2 N / 3kT) \left[\sum_{S=0}^5 (2S+1)S(S+1) \exp[-JS(S+1) / 2kT] \right] / \left[\sum_{S=0}^5 (2S+1) \exp[-JS(S+1) / 2kT] \right] (1 - \rho) + [35\beta^2 N / 3k(T - \Phi)] \rho \quad (3)$$

with which to investigate angular dependence of antiferromagnetic coupling in molecules where the bridge angle is the a priori dominant variable.

The temperature dependencies of the magnetic susceptibilities of the two complexes are plotted in Figures 4 and 5. Detailed analyses of the magnetism of these compounds have been performed, and existing susceptibility data for [Fe(salen)]₂O²⁶ and [Fe(salen)]₂S⁷ have been reanalyzed in a consistent manner to permit a meaningful comparison of J values of the four compounds. In all cases the paramagnetic impurity clearly evident at low temperatures has been treated as a high-spin Curie or Curie-Weiss ($\chi^{\text{M}} = C / (T - \Phi)$) Fe(III) contribution. Fits are sensitive to diamagnetic corrections, which are dominated by the salen or salen portion of the ligands. In this work we have adopted the measured value of H₂(salen) by Belova and Syrkin³⁶ because of its internal consistency with other measurements of similar compounds. The measured value applied earlier to [Fe(salen)]₂S⁷ is substantially different.⁴⁶ The best-fit parameters obtained by using the Simplex method⁴⁷ and the function minimized for best fit are contained in Table VI. In the various calculations, two, three or all of the parameters J , ρ , g , and Φ were allowed to float in order to investigate the variability of J . The determined J values fall into rather narrow ranges except for those of [Fe(3-*t*-Busaltmen)]₂S where the spread is 21 cm⁻¹. Given the presence of high-spin Fe(III), we prefer the best-fit values with g constrained to the free electron value.

The best-fit J values lead to the following conclusions. (vi) Antiferromagnetic coupling through oxo and sulfido bridge atoms is dependent on the bridge angle, although the effect is not large. An increase of 9% in J arises by enlarging the Fe-O-Fe angle by 29° and an increase of 22% is found upon opening the Fe-S-Fe angle by 45°. (vii) Inasmuch as θ values for the pair 6/7 differ

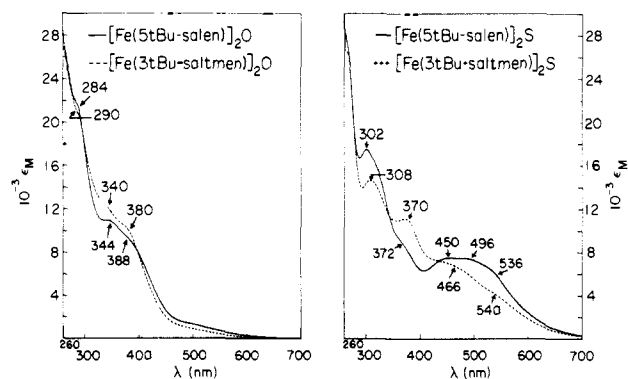


Figure 6. Absorption spectra of μ -oxo and μ -sulfido complexes in dichloromethane solutions; positions (nm) of band shoulders and maxima are indicated.

by only 6.4°, at constant Fe-X-Fe angle and similar conformations coupling through a sulfido bridge is larger than through an oxo bridge.

Conclusion vi could not be securely drawn from the existing body of magnetic results, although extensive, owing to difficulties such as limited temperature intervals of measurement, different methods of data analysis, inconsistent corrections for paramagnetic impurities, use of calculated ligand susceptibilities, unequal Fe-O bridge bond distances, and differing ligand systems.⁴⁸ These problems have been reduced or eliminated in the present work. In particular, Fe-O bridge distances are indistinguishable to the level of 1 σ in 6 and 8. Larger variations in J should follow when the range of bridge angles is expanded. Conclusion vii could not be established (although it was inferred⁷) from the previously investigated pair 8/9 because of the 23° difference in bridge angle. Given the large Fe...Fe separations, especially in 6/7, it is improbable that direct metal-metal interactions contribute significantly to the magnetic coupling. Members of the pair 10/11 are antiferromagnetically coupled,⁸ but detailed data have not been reported.

Solution Structures and Properties. Solution behavior has been examined with soluble salen complexes 4, 5, and 8 and with saltmen complexes 6 and 7. The extreme sensitivity of the sulfido bridged complexes to protic impurities and dioxygen and the tendency toward autoreduction are emphasized. These were not always appreciated in our earlier study,⁷ and considerable care has been taken here to avoid decomposition. These compounds are best examined in rigorously dry and dioxygen-free solvents. Sulfido-bridged complexes react slowly with chlorinated solvents to form high-spin chloro complexes. An immediate question is whether or not the solid-state structures in Figures 1 and 2 and Table V are retained in solution.

(a) Absorption Spectra. The spectra in Figure 6 reveal differences in the bridge atom \rightarrow Fe(III) LMCT region, which are particularly pronounced with the sulfido-bridged complexes and imply a difference in structure between salen and saltmen complexes with the same bridge atom. The spectra are otherwise of value in being the simplest means to identify the complexes in question. The spectrum previously attributed to [Fe(salen)]₂S in DMF⁷ is actually that of the autoredox product Fe(salen)-(DMF)₂.

(b) Magnetism. Previously we have shown for different compounds that retention of the same extent of antiferromagnetic coupling as in the solid permits a choice between structures with different J values.⁴⁹ This approach has been taken with [Fe(3-*t*-Busaltmen)]₂O and [Fe(salen)]₂O, whose magnetic properties in the solid state and in dichloromethane solution are graphically

(46) $\chi^{\text{M}} = -182 \times 10^{-6}$ cgsu: Bayer, E.; Bielig, H.-J.; Hausser, K. H. *Ann.* **1953**, *584*, 116.

(47) (a) Caceci, M. S.; Cacheris, W. P. *Byte* **1983**, *9*, 340. (b) Nedler, J. A.; Mead, A. *Comput. J.* **1965**, *7*, 308.

(48) As one example of this effect, variation of phenyl ring substituents in a set of μ -oxo iron(III) tetraphenylporphyrinate complexes causes small changes in J : Helms, J. H.; ter Haar, L. W.; Hatfield, W. E.; Harris, D. L.; Jayaraj, K.; Toney, G. E.; Gold, A.; Mewborn, T. D.; Pemberton, J. R. *Inorg. Chem.* **1986**, *25*, 2334.

(49) Whitener, M. A.; Bashkin, J. K.; Hagen, K. S.; Girerd, J.-J.; Gamp, E.; Edelstein, N.; Holm, R. H. *J. Am. Chem. Soc.* **1986**, *108*, 5607.

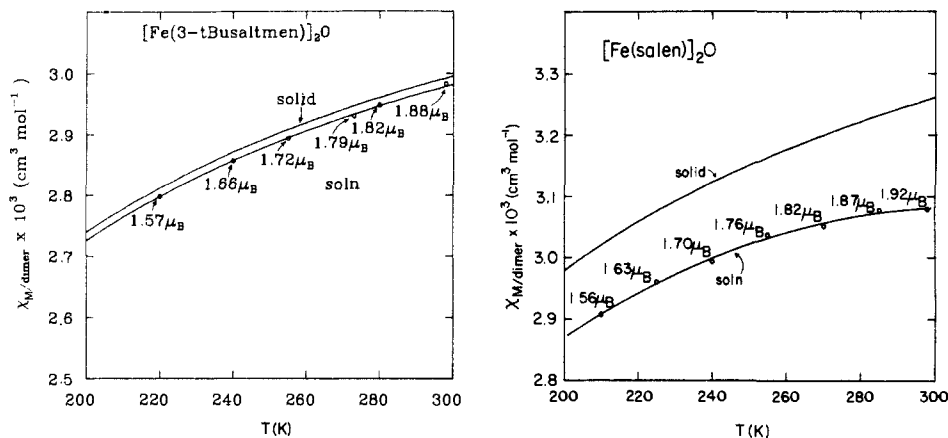


Figure 7. Comparison of molar susceptibilities of $[\text{Fe}(3\text{-}t\text{-Busaltmen})]_2\text{O}$ (6, left) and $[\text{Fe}(\text{salen})]_2\text{O}$ (8, right) in the solid state and in dichloromethane solution. The solid-state curves are theoretical fits to the data with $J = -200 \text{ cm}^{-1}$ (6) and -183 cm^{-1} (8). The solution curves are also fits, based on the parameters in Table VII. Magnetic moments per Fe atom in solution, calculated from the Curie law, are indicated.

Table VII. Solution Magnetic Properties of $\mu\text{-X}$ Complexes ($\text{X} = \text{O}, \text{S}$)

complex	solvent	$\mu_{\text{eff}}/\text{Fe}^a$ (μ_B)	J^b (cm^{-1})	a_i (G)			
				$a_1^{3\text{-H}}$	$a_2^{3\text{-H}}$	$a_1^{4\text{-H}}$	$a_2^{4\text{-H}}$
$[\text{Fe}(\text{salen})]_2\text{O}$	CD_2Cl_2	1.92	-191 (2)	-0.057	-0.082	0.059	0.074 ^f
$[\text{Fe}(3\text{-}t\text{-Busaltmen})]_2\text{O}$	CD_2Cl_2	1.88	-201 (2)			0.061	0.098
	Me_2SO	<i>c</i>	<i>d</i>			0.078	0.034
$[\text{Fe}(3\text{-}t\text{-Busaltmen})]_2\text{S}$	Me_2CO	<i>c</i>	-218 ^e			0.074	0.090

^a 298 K. ^b Uncertainties were determined by assuming uncertainties on T ($\pm 2 \text{ K}$) and χ^M ($\pm 5\%$) and applying a sensitivity test to the original data; multiple data sets were generated by randomly varying each data point within the assumed uncertainties. The stated uncertainties represent standard deviations of fits to all data sets. ^c Not measured. ^d Value in CD_2Cl_2 assumed. ^e Solid-state value; see text. ^f $a_1^{5\text{-H}} = -0.033 \text{ G}$, $a_2^{5\text{-H}} = -0.068 \text{ G}$.

compared in Figure 7. Solid-state data are presented as theoretical fits to eq 3 with the indicated J values. Solution susceptibilities were determined at six or seven temperatures in the 210–298 K range. It is immediately apparent that both compounds retain their antiferromagnetism in solution. This behavior has been shown previously for $[\text{Fe}(5\text{-}t\text{-Busalen})]_2\text{O}$.⁵⁰

For $[\text{Fe}(3\text{-}t\text{-Busaltmen})]_2\text{O}$, the temperature dependencies of susceptibilities in the two phases closely parallel each other. The situation with $[\text{Fe}(\text{salen})]_2\text{O}$ is similar, but at all temperatures the compound is somewhat *less* paramagnetic in solution than in the solid state. At 298 K, the solution susceptibility is 6% less than that in the solid.⁵¹ Both solution data sets were fit to eq 3 with the Simplex method. The same fractions of paramagnetic impurity as found in solid samples were assumed. Excellent fits were obtained; resultant J values are given in Table VII together with their estimated uncertainties.⁵² Comparison with the results in Table VI reveals that the J values for $[\text{Fe}(3\text{-}t\text{-Busaltmen})]_2\text{O}$ in the crystalline state and dichloromethane solution are effectively identical. This demonstrates no important structural change in solution, a situation consistent with the narrow range of stable bridge angles allowed by nonbonded interactions (Figure 3). For $[\text{Fe}(\text{salen})]_2\text{O}$, the solution value is slightly higher than the solid-state value. Such behavior shows that if any structural change occurs in solution, it is the opening of the bridge angle, but certainly not near the 173° value of 6.

Despite numerous attempts under rigorously anaerobic conditions with purified solvents (including, e.g., dry toluene), reliable solution susceptibilities of sulfido-bridged complexes could not be obtained. The data were consistently suggestive of the presence of high-spin impurities, which are otherwise readily formed by

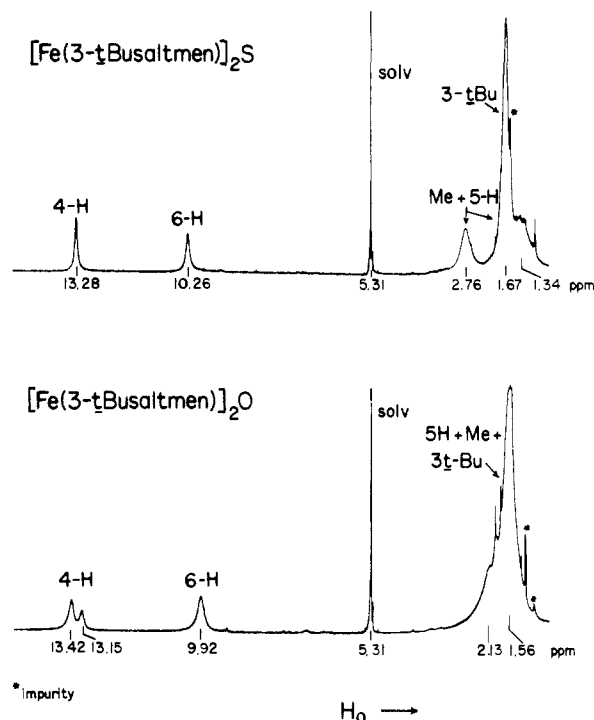


Figure 8. ^1H NMR spectra of $[\text{Fe}(3\text{-}t\text{-Busaltmen})]_2\text{O}$ and $[\text{Fe}(3\text{-}t\text{-Busaltmen})]_2\text{S}$ in dichloromethane solutions at $\sim 25^\circ\text{C}$; signal assignments, chemical shifts, and impurities (*) are indicated.

protic cleavage of the bridge or autoredox.

^1H NMR Spectra. Analysis of the spectra of $[\text{Fe}(\text{salen})]_2\text{O}$ and certain derivatives and the basic theory of contact shifts in antiferromagnetically coupled dimers have been given earlier.⁵⁰ Spectra have been investigated here to ascertain if spin density distributions are influenced to a detectable extent by bridge atom and bridge angle variations. Spectra of the two $[\text{Fe}(3\text{-}t\text{-Busaltmen})]_2\text{X}$ complexes are shown in Figure 8; those of $[\text{Fe}(\text{salen})]_2\text{X}$ are available elsewhere.⁷ The doubled 4-H signal of 6 persists in Me_2SO solution up to 383 K. It is ascribed to a locked con-

(50) La Mar, G. N.; Eaton, G. R.; Holm, R. H.; Walker, F. A. *J. Am. Chem. Soc.* 1973, 95, 63.

(51) In treating the magnetic data of $[\text{Fe}(\text{salen})]_2\text{O}$ in the solid state (Table VI and Figure 7), it has been assumed that the sample measured was *not* solvated although Wollman and Hendrickson²⁶ report purification by recrystallization from dichloromethane. Their analytical data are consistent with the unsolvated form. In our hands, we have been unable to desolvate $[\text{Fe}(\text{salen})]_2\text{O}\cdot\text{CH}_2\text{Cl}_2$, a compound reported much earlier,²¹ without decomposition.

(52) A change in the paramagnetic impurity by +0.5% causes a larger change in J than do estimated uncertainties in Table VII. The J values given are lower limits.

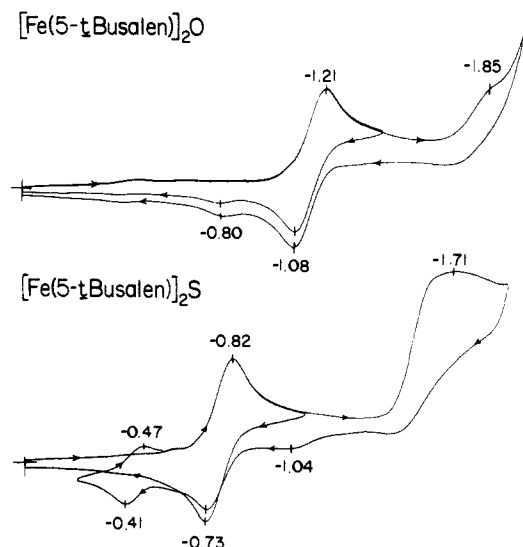


Figure 9. Cyclic voltammograms of $[\text{Fe}(5\text{-}t\text{Busalen})]_2\text{O}$ (upper) and $[\text{Fe}(5\text{-}t\text{Busalen})]_2\text{S}$ in dichloromethane solutions at 25 °C and a scan rate of 50 mV/s. Peak potentials versus SCE are indicated.

formation of the two half-dimers, which arises from steric interactions among 3-*t*Bu and bridge methyl groups. (Note the lack of symmetry in the solid-state structure.) All ring proton signals in the spectrum of **7** are singlets, indicating free rotation.

Contact shifts of complexes **6–8** were determined in CD_2Cl_2 and/or acetone- d_6 solutions at 210–300 K.⁵³ In all cases, alternating signs of ring proton shifts and positive contact shifts of 3-H and 5-H (where observable) are consistent with dominant contact shifts and ligand \rightarrow metal antiparallel spin transfer.⁵⁴ Contact shifts of 4-H and/or 3-H of the three complexes in Table VII were fit to eq 4 by using solution J values for **6** and **8**. In this equation, $P = g\beta/6\gamma_H\hbar k$ and the symbols have their usual meanings. Given the results for **6** and the inability to obtain highly

$$\left(\frac{\Delta H}{H_0}\right)_{\text{con}}^i = \frac{P}{T} \frac{\sum_{i=0}^5 a_i (2S_i + 1) S_i (S_i + 1) \exp(-E_i/kT)}{\sum_{i=0}^5 (2S_i + 1) \exp(-E_i/kT)} \quad (4)$$

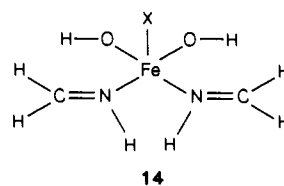
accurate solution susceptibilities, the solid-state J value was assumed for **7**. Resonances of 5-H were not always resolved from other signals and the temperature dependence of the 6-H chemical shift was too small for meaningful fitting. Two-parameter fits proved adequate. The coupling constants, given in gauss in Table VII, are sensibly consistent for the two oxo complexes and not sufficiently different from those for **7** to signify a real effect of bridging atom on π -spin delocalization. On this basis, it would appear that the larger contact shifts previously shown for $[\text{Fe}(\text{salen})]_2\text{S}$ versus $[\text{Fe}(\text{salen})]_2\text{O}$ ⁷ arise mainly from differences in susceptibilities than in spin densities. This interpretation is reinforced by any opening of the oxo bridge angle in solution, which would increase antiferromagnetic coupling.

Voltammetry. In dichloromethane solutions, $[\text{Fe}(5\text{-}t\text{Busalen})]_2\text{O}$ and $[\text{Fe}(5\text{-}t\text{Busalen})]_2\text{S}$ show chemically reversible one-electron reductions at $E_{1/2} = -1.15$ and -0.78 V versus SCE, respectively. Voltammograms are presented in Figure 9. As with $[\text{Fe}(\text{salen})]_2\text{O}$ in Me_2SO ,⁵⁵ which behaves analogously, these reductions afford the mixed valence Fe(II,III) complexes. The one-electron reduction of **5** was confirmed in acetone by controlled potential coulometry. In each case, a second reduction is observed at more negative potentials and is irreversible. The feature at -0.80 V in the voltammogram of **4** arises from the oxidation of a small

amount of $[\text{Fe}(5\text{-}t\text{Busalen})(\text{OH})]^{1-}$.⁵⁶ For the couple $[\text{Fe}(\text{salen})(\text{OH})]^{-0}$, $E_{1/2} = -0.70$ V in Me_2SO .⁵⁵ In the case of **5**, the reversible oxidation at $E_{1/2} = -0.44$ V following the cathodic scan to -1.8 V is due to the couple $[\text{Fe}(5\text{-}t\text{Busalen})\text{Cl}]^{-0}$. The Fe(III) complex was formed from the reaction of solvent with $\text{Fe}(\text{salen})$, which arises in the irreversible reduction near -1.7 V and is reduced to the monoanion⁵⁶ at that potential.⁵⁷ The reduction of $[\text{Fe}(3\text{-}t\text{Busaltmen})]_2\text{O}$ occurs as a broad quasireversible feature near -1.50 V, while that of $[\text{Fe}(3\text{-}t\text{Busaltmen})]_2\text{S}$ is irreversible with $E_{p,c} = -1.05$ V. No other reductions were observed out to -2.0 V.

Two main results emerge from these experiments. (i) Potentials for sulfido complexes are less negative than those for analogous oxo complexes. This is the first observation of this effect for bridged Fe complexes and is another manifestation of the consistent trend $E(\text{S}) > E(\text{O})$ for analogous complexes differing only in anionic S/O ligand replacement.⁵⁸ (ii) The bridge units Fe–O–Fe and Fe–S–Fe are more difficult to reduce at larger bridge angles.⁵⁹

Electronic Structural Preferences. Having shown that structures of complexes **6–9** in solution, where we assume the lowest energy molecular configurations, are the same as, or similar to, those in the crystalline state, we conclude by examining structural preferences based on relative electronic energies. This has been done with MO calculations performed at the extended Hückel level, and utilizing **14** with C_{2v} symmetry as the calculational model for a half-dimer. For X = O, Fe–O, Fe–N, and C–N distances and



out-of-plane displacement δ were average values from the structure of **8**.²² For X = S, the preceding distances were used and δ was the mean value of **9**. The Fe–X distances were mean values of **6** and **8**, or **7** and **9**. The remaining distances were standard values, bond angles at Fe were taken as 90°, and angle Fe–O–H = 132°. The z-axis is along Fe–X, and the x- and y-axes bisect bond angles at the Fe atom.

With atom X absent and the Fe atom in the coordination plane, the d-orbital energy order is $xy \gg x^2 - y^2 > yz \gtrsim z^2 \gtrsim xz$. The out-of-plane order is $xy \gg yz \gtrsim xz > x^2 - y^2 > z^2$. Two structural variables were investigated: conformations and bridge angles. Certain of the calculations resemble those by Tatsumi and Hoffmann^{38a} in their pertinent study of a D_{2d} model of a μ -oxo bis[iron(III) porphyrinate], $[\text{Fe}(\text{P})]_2\text{O}$. The present results are somewhat more involved owing to the lower symmetry of the bridged model and the attendant lack of orbital degeneracy.

(a) Conformations. This property was investigated for linear bridges. The variable is the rotational angle Ω about the Fe–X–Fe bridge; when $\theta = 180^\circ$, $\Omega = \Omega_1 + \Omega_2$. As seen from the plot in Figure 10, the X = S species is most stable in the C_{2v} , and least stable in the C_{2h} , conformation. The destabilization energy is not large, about 4 kcal/mol. The Walsh diagram provides the basic d-block energy scheme for sulfido-bridged complexes. The most stable ($1a_1 + 1b_1$) and least stable ($4a_1 + 4b_1$, omitted) orbitals are δ -type MO's; dominant components of the intermediate orbitals are depicted. Upon passing to the C_{2h} conformer, only the HOMO

(56) In acetonitrile $\text{Fe}(\text{salen})$ reacts immediately with a number of anionic ligands L, including Cl^- , OH^- , and RS^- , to form the complexes $[\text{Fe}(\text{salen})\text{L}]^-$, which have been isolated as R_4N^+ salts. For the couple $[\text{Fe}(\text{salen})(\text{OH})]^{-0}$ in dichloromethane, $E_{p,a} = -0.69$ V.

(57) The potential of the $[\text{Fe}(\text{salen})]_2\text{S}^{0-}$ was misreported as -1.27 V;⁷ the correct value is -0.67 V. The oxidation claimed for this compound at -0.28 V⁷ is actually the oxidation of its autoredox product $\text{Fe}(\text{salen})(\text{DMF})_2$.

(58) For a partial list of comparative potentials, cf.: Harlan, E. W.; Berg, J. M.; Holm, R. H. *J. Am. Chem. Soc.* **1986**, *108*, 6992.

(59) Substituent effects cannot fully account for the more negative potentials; in acetonitrile potentials for the couples $[\text{Fe}(\text{salen})\text{Cl}]^{0-}$ and $[\text{Fe}(3\text{-}t\text{Busaltmen})\text{Cl}]^{0-}$ are -0.41 and -0.52 V, respectively.

(53) Contact shifts were evaluated from $(\Delta H/H_0)_{\text{con}} = (\Delta H/H_0)_{\text{dia}} - (\Delta H/H_0)_{\text{obsd}}$, where the diamagnetic shifts are those of the free ligands.

(54) La Mar, G. N. In *NMR of Paramagnetic Molecules*; La Mar, G. N., Horrocks, W. D., Holm, R. H., Eds.; Academic: New York, 1973; Chapter 3.

(55) Wenk, S. E.; Schultz, F. A. *J. Electroanal. Chem.* **1979**, *101*, 89.

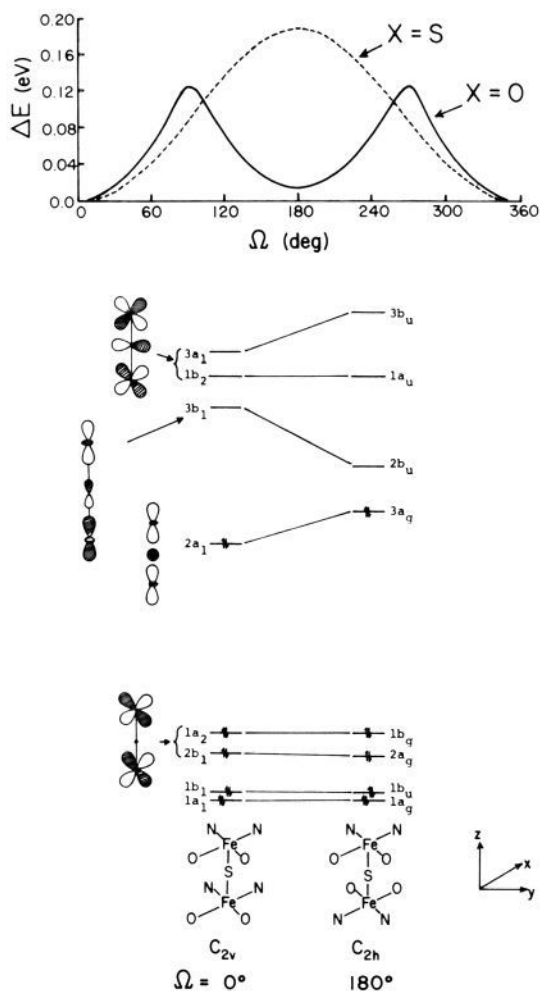


Figure 10. Relative energies of $[\text{Fe}(\text{OH})_2(\text{H}_2\text{CNH})_2]_2\text{X}$ ($\text{X} = \text{O}, \text{S}$) as dependent on conformational angle Ω at $\theta = 180^\circ$, and a Walsh diagram for $\text{X} = \text{S}$ correlating the $\Omega = 0^\circ$ and 180° conformations. Principal d-orbital contributions to selected MO's are depicted.

($2a_1$) which becomes $3a_g$ experiences a significant energy change. Its destabilization (by 2.4 kcal/mol) is the likely cause of the relative instability of the C_{2h} conformer. Inasmuch as the $d_{z^2}/3s$ bridge interaction is independent of Ω , the effect is somewhat subtle, and may reside in the core levels below the d-block. The 3d composition of $3a_g$ (72%) versus that of $2a_1$ (65%) reflects this possibility. Bridge atom orbitals contribute only very slightly (<4%) to the MO's.

The oxo-bridged model is essentially equally stable at $\Omega = 0^\circ$ and 180° and somewhat destabilized at $\Omega = 90^\circ$ (by 3 kcal/mol). In the C_{2v} limit the HOMO is a π^* orbital of b_1 symmetry (mainly $d_{xz} + 3p_x - d_{xz}$) and the LUMO is the analogous b_2 orbital. In going over to the C_2 90° form, there is substantial orbital mixing and the HOMO is raised by about 1.6 kcal/mol, the probable source of destabilization.

Of the complexes in Table V, only **6** and **7** approach the linear bridge arrangement. In the limit of $\theta = 180^\circ$, $\Omega \approx -102^\circ$ and 261° may be estimated for **6** and **7**, respectively. While the energy differences are small, the conformations of both compounds are clearly well removed from the positions of minimum energy predicted for the singlet state.

(b) Bridge Angles. Calculations were performed with variable θ at a large number of $[\Omega_1, \Omega_2]$ values, affording a partial energy surface. The necessity of examining the effects of the latter angular variables is made evident by the differences in conformational energies at $\theta = 180^\circ$, and the possibility in real molecules of bending the bridge at any set of values of these angles. The results in Figure 11 reveal the usual behavior. Here calculations were carried out for the six compounds in Table V by using

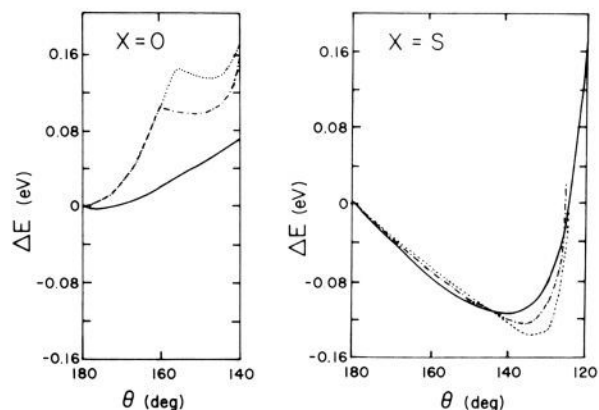


Figure 11. Relative energies at $[\text{Fe}(\text{OH})_2(\text{H}_2\text{CNH})_2]_2\text{X}$ ($\text{X} = \text{O}, \text{S}$) as dependent on bridge angle θ at fixed conformational angles Ω_1 and Ω_2 for complexes **6**–**11**: —, $[\text{Fe}(\text{3-}t\text{Busaltmen})_2]_2\text{X}$; ---, $[\text{Fe}(\text{salen})_2]_2\text{X}$; -·-·-, $[\text{Fe}(\text{acen})_2]_2\text{X}$.

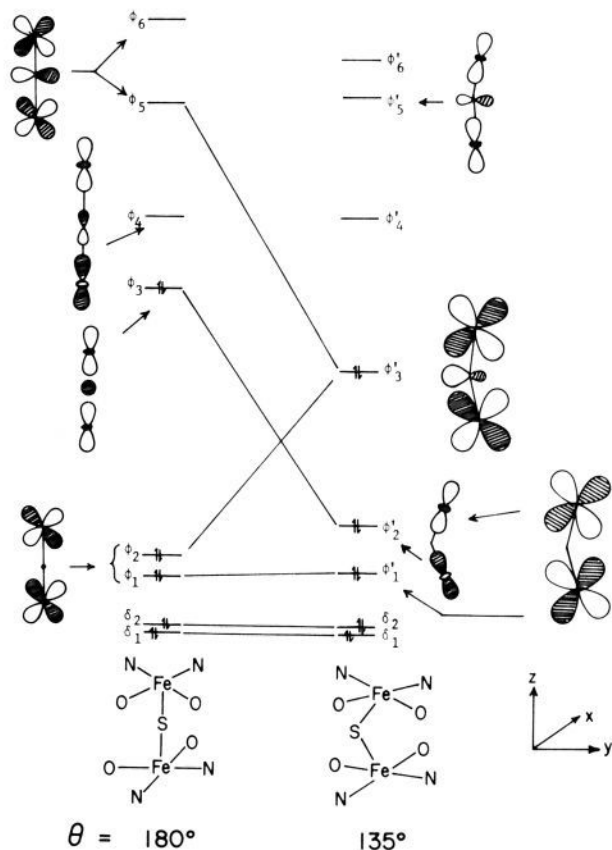


Figure 12. Orbital energy level scheme for $[\text{Fe}(\text{OH})_2(\text{H}_2\text{CNH})_2]_2\text{S}$ showing the dependence on bridge angle at $\theta = 180^\circ$ and 135° . The crystalline state conformation $[\Omega_1, \Omega_2]$ of $[\text{Fe}(\text{salen})_2]_2\text{S}$ (Table V) was assumed at both angles. In some cases, orbital depictions and correlations are quite approximate due to significant orbital mixing in the C_2 symmetry of both forms.

crystallographic values of the conformational angles. For $\text{X} = \text{O}$, the energy minimum occurs at or very close to $\theta = 180^\circ$. Maximum destabilization, 3.7 kcal/mol, is found in the conformations of **8** and **10**; the conformation of **6** is somewhat less destabilizing as the angle is closed. For $[\text{Fe}(\text{P})_2\text{O}]$, the apparent minimum energy bridge is nonlinear^{38a} ($\theta \approx 150^\circ$), but the energy profile is even softer than here. In the case of $\text{X} = \text{S}$, energy minima are found at 135 – 140° with stabilization energies of about 3 kcal/mol.

Orbital energy changes pursuant to bending the bridge of the model of $[\text{Fe}(\text{salen})_2]_2\text{S}$ are depicted in Figure 12. As θ is decreased below 180° , orbital mixing in the d-block is quite pro-

nounced for some levels and the depictions of dominant contributions are rather qualitative. Nonetheless, some orbital correlations emerge. The orbitals of main importance are Φ_2 and Φ_3 in the linear case and Φ_2' and Φ_3' in bent geometry. Orbital Φ_3 (65% d_{z^2}) passes to Φ_2' , which is a combination of d_{z^2} (51%) and d_{xz} (26%); it appears to be less antibonding because of the absence of any significant sulfur orbital contribution. Orbital Φ_3' from Φ_2 is more antibonding because of interaction with the bridge sp hybrid orbital. The overriding effect is that the HOMO is stabilized more in the bent (Φ_3') than in the linear (Φ_3) arrangement. The situation with $\text{X} = \text{O}$ is less clear. The HOMO is π -antibonding to S 3p orbitals in both arrangements and its energy is nearly constant. The next orbital down, which approximates ($d_{xz} + d_{zz}$) at $\theta = 180^\circ$, becomes strongly mixed with d_{z^2} on bending and is destabilized. This energy change may be significant in resisting bending.

The least sterically hindered complexes of the $\text{X} = \text{O}$ set, **8** and **10**, with bridge angles of about 145° and 151° , respectively, are displaced from the linear arrangement predicted by the MO treatment. On the other hand, the analogously least hindered $\text{X} = \text{S}$ complexes **9** and **11** have decidedly bent bridges as predicted, but with somewhat more acute angles ($\theta = 121\text{--}122^\circ$). From these results we conclude that with the oxo-bridged complexes nonbonded interactions override bridge angle preference. Except when sterically forced, the bridges are nonlinear. With sulfido-bridged complexes, bridge angle preference and the effects of nonbonded interactions reinforce, the result being stabilization of strongly bent bridge. Because of the approximate nature of the calculations, we cannot meaningfully apportion opposing or conflicting nonbonded repulsive and electronic structural preferences.

A practical MO theory of coupling through a single bridge atom has been developed by Hay et al.²⁵ for a symmetrical dimer in which each metal has n unpaired electrons. Considering only antiferromagnetic interactions, which are dominant for the present complexes, the coupling constant is approximated by $J = -(1/n^2) \sum_{i=1}^n \Delta_i^2 / U_i$, where the sum extends over all magnetic orbitals n , U_i is an interelectron repulsion parameter on each metal, and Δ_i is the energy separation of d-type MO's. In previous work on the $[\text{Fe}(\text{P})]_2\text{O}$ model,^{38a} the orbitals that vary the most with bridge angle are of the form $\Phi_S = (d_{xz} + p_z - d_{zz})$ and $\Phi_A = (d_{xz} + d_{zz})$ (depending on choice of coordinates), and their energy separation decreases with decreasing bridge angle. The same trend is evident here from calculations on the $\text{X} = \text{O}$ and S cases. One instance is seen in Figure 12 for magnetic orbitals of substantial d_{xz} character. While a more rigorous treatment of the angular dependence of J is desirable, it is seen that J values do decrease as the bridge angle departs from linearity for both oxo and sulfido bridges.

In presenting the foregoing observation as well as the results in Figure 11, we are aware that $[\Omega_1, \Omega_2]$ and θ will simultaneously vary along a least-energy pathway. The nonbonded repulsion energy calculations in Figure 3 tend to substantiate this. We have not obtained detailed surfaces of total electronic or individual orbital energies as dependent on the three angular variables, considering the calculations as too approximate to justify such an extensive effort. Instead, we offer results based on reasonable parameter restrictions which we consider to have significance in a relative sense. With regard to antiferromagnetic coupling, it should be noted that there is no experimental information on the effects of conformational variation at constant θ on J . Our conclusions have emphasized the role of the bridge angle itself in modulating coupling interactions.

Summary. The following are the principal findings and conclusions of this investigation.

(1) At parity of terminal ligand structure, the bridge angles Fe-X-Fe ($\text{X} = \text{O}, \text{S}$) containing high-spin Fe(III) fall in the order $\text{X} = \text{S} < \text{O}$ and respond to nonbonded interactions between half-dimers.

(2) Conformations of $\mu\text{-X}$ complexes containing a single bridge and half-dimers of two fold symmetry are completely definable in terms of bridge angle θ and two conformational angles $[\Omega_1, \Omega_2]$ which specify the relative orientations of the halves.

(3) Antiferromagnetic spin coupling increases as bridge angle increases. No other data are available to test the dependence of J on θ ; conformational angles are not constant over these ranges. Bridge Fe-O distances are indistinguishable in **6** and **8**, and therefore are not a factor in regulating coupling. The J values of **6** and **7** constitute the best current evidence, at least for high-spin Fe(III), that at (near-) constant θ antiferromagnetic coupling is transmitted more effectively by a sulfido than an oxo bridge.

(4) On the basis of J values obtained from analysis of magnetic susceptibilities, complexes **6** and **8** retain their solid-state structures in solution, although possibly the bridge angle of **8** opens somewhat. The larger contact shifts of **9** versus **8** appear, from evaluations of hyperfine coupling constants, to arise mainly from susceptibility differences traceable to different bridge angles, than to important divergences in spin density distributions owing to non-identical bridge atoms.

(5) The configurations of complexes **6-11** are predicted within small limits of angular parameters by use of the van der Waals potential function 2 (Figure 3). Structural preferences based on relative electronic energies assessed at the EHMO level with half-dimer model **14** include (i) the conformations $\Omega = \Omega_1 + \Omega_2 = 0^\circ$ or 180° ($\text{X} = \text{O}$) and 0° ($\text{X} = \text{S}$) at $\theta = 180^\circ$, and (ii) $\theta \approx 180^\circ$ ($\text{X} = \text{O}$) and $135\text{--}140^\circ$ ($\text{X} = \text{S}$) at crystallographic $[\Omega_1, \Omega_2]$ angles. Departure of **6** and **7** from (i) and **8** and **10** from (ii) indicates that nonbonded repulsion energies override electronic structural preferences, which are generally small (≤ 4 kcal/mol). Nonbonded effects and preference ii act in concert with **9** and **11**, affording markedly bent bridges. Deformation of **6** and **7** from the structures **8** and **9**, respectively, clearly arises entirely from steric repulsion.

(6) Increasing J values with increasing θ conforms to a conceptually useful MO model of antiferromagnetic interactions.²⁵ Magnetic bridge orbitals whose energy changes are mainly responsible for the effect are of the π -antibonding type, corresponding to a π -superexchange pathway.

Acknowledgment. This research was supported by National Institutes of Health Grant 28856. X-ray equipment was obtained by National Institutes of Health Grant 1-S10-RR-02247. We thank M. J. Carney and J. C. Choi for experimental assistance and Prof. D. M. Hoffman for useful discussions.

Registry No. **4**, 112714-07-5; **5**, 112714-08-6; **6**, 112714-05-3; **7**, 112714-06-4.

Supplementary Material Available: Positional and thermal parameters, hydrogen atom positional parameters, interatomic distances and angles, stereoviews, and magnetic susceptibilities for **6** and **7**; recalculated magnetic susceptibilities for **8** and **9**; and magnetic susceptibility fitting parameters for **6-9** (24 pages); listing of calculated and observed structure factors (46 pages). Ordering information is given on any current masthead page.